An-Najah National University

Faculty of Graduate Studies

Synthesis, Spectral, Thermal, Electrochemical Characterization of New Family of Semi-Octahedral Diamine / Copper (II) Complexes and their Biological Activities

By

Bahaa Abd Al-Ghani

Supervisor

Prof. Ismail Warad

This Thesis is Submitted in Partial Fulfillment of the Requirements for the Degree of Master of Chemistry, Faculty of Graduate Studies, An-Najah National University, Nablus, Palestine.

2017

Synthesis, Spectral, Thermal, Electrochemical Characterization of New Family of Semi-Octahedral Diamine / Copper (II) Complexes and their Biological Activities

By

Bahaa Abd Al-Ghani

This Thesis was defended successfully on 20/6/2017 and approved by:

Defense Committee Members	**Signature**
– **Prof. Ismail Warad / Supervisor**	.....
– **Dr. Nizam Diab / External Examiner**	.....
– **Prof. Mohammed A. Al-Nuri/ Internal Examiner**	.....
– **Dr. Ashraf Swaftah/ Internal Examiner**	.....

Dedicated To

My Affectionate Parents,

Brothers And Sisters.

Special Dedication To

My Father ,AliAbdAl-Ghani

My Mother Amenah

My Wife ,Falasteen

My Son ,Yaman, and

My daughter Aleen.

With my Respect and Love.

Acknowledgments:

I would like to express my deep appreciation and respect to Prof. Ismail warad(Advisor) for his direct supervision, encouragement and help throughout the course of this work. Also , I would like to thank my committee members, Prof. Mohammed Al-Nuri , Dr.Nizam Diab and Dr. Ashraf Swafta for their fruitful discussions.Special thanks are due to my father, Ali , my mother, Amenah , and my wife, Falasteen , for their support and encouragement. Special thanks are extended to my brothers Nofal andMohammad,And to my sisters, Bothaina, Arwa ,Maisaa,Tasneem, and Sojoud,and to my kids Yaman , Aleen and wisam.Thanks are also extended to my friends and to Mr. Nafith Dwikat for his helping and support during my work in the laboratory.

الإقرار

أنا الموقع أدناه مقدم الرسالة التي تحمل العنوان

Synthesis, Spectral, Thermal, Electrochemical Characterization of New Family of Semi-Octahedral Diamine / Copper (II) Complexes and their Biological Activities

أقر بأن ما شملت عليه الرسالة هو نتاج جهدي الخاص, باستثناء ما تمت الإشارة إليه حيثما ورد، وأن هذه الرسالة ككل أو أي جزء منها لم يقدم من قبل لنيل أي درجة أو لقب علمي أو بحثي لدى أي مؤسسة علمية أو بحثية

Declaration

The work provided in this thesis, unless otherwise referenced, is the researcher's own work, and has not been submitted elsewhere for any other degrees or qualifications.

Student's Name: **اسم الطالب:**

Signature **التوقيع:**

Date **التاريخ:**

List of Contents

List of Figures

List of Tables

List of Abbreviation

Symbol	Abbreviation
IR	Infrared spectroscopy
UV-Vis	Ultraviolet–visible spectroscopy
TG	Thermogravimetric analysis
EA	Elemental Analysis
MS	Mass Spectroscopy
CV	Cyclic voltammetry
XRD	X-Ray Diffraction
EDX	Energy-dispersive X-ray spectroscopy
SEM	Scanning electron microscope
EPR	Electron paramagnetic resonance
DFT	Density Functional Theory
FT-IR	Fourier transform infrared spectroscopy
NMR	Nuclear magnetic resonance spectroscopy
EI-MS	Electron ionization Mass Spectroscopy
CCD Diffractometer	Bruker AXS SMART APEX CCD X-Ray Diffractometer
*T*HF	Tetrahydrofuran
MW	Microwave
$CDCL_3$	Deuterated chloroform
TMS	Tetramethylsilane
m.p.	Melting Point
R	Reflection coefficient
$Cu_{K\alpha}$	X-ray notation of Copper
RPMI	Roswell Park Memorial Institute medium
HCT116	colon cells in Human
HepG2	epithelial cells of the liver in Human
DMED	Dulbecco’s modified Eagle’s medium
PC3	human prostate cancer cells
DN	Gutmann’s donor values
ε_f	Free Complex Extinction Coefficient
ε_a	Apparent Complex Extinction Coefficient

ε_b	Bound Complex Extinction Coefficient
K_b	equilibrium binding constant
IC_{50}	half maximal inhibitory concentration
CT-DNA	Circulating tumor DNA
DMSO	Dimethyl sulfoxide
DMF	Dimethylformamide
H_2O	Water
EtOH	Ethanol
CuO	Copper Oxide
MTT assay	colorimetric assay for assessing cell metabolic activity
[DNA]	Concentration of DNA
OD	optical density
3D	Three-Dimensional
2D	Two- dimensional
ATCC	The Global Bioresource Center

Synthesis, Spectral, Thermal, Electrochemical Characterization of New Family of Semi-Octahedral Diamine / Copper (II) Complexes and their Biological Activities

By
BahaaAbd Al-Ghani
Supervisor
Prof. Ismail Warad

Abstract

Our research focuses on synthesis of novel compounds which are expected to be excellent donating compounds in coordination chemistry besides synthesis of their complexes.

Four new hydrated monocationCu(II) complexes with 1,3-propylenediamine and1,2-ethylenediamine with chloro or bromo ligands were prepared in acceptable yield. The complexes were spectrally characterized by (IR, UV-visible, and TOF-MS) as well as by thermal (TG/DTA) and elemental analysis. The three dimensional structure for complexes **2,4**were proved by X-ray diffraction studies, which show the Cu(II)is coordinated by four nitrogen atoms of the base ligand and one bromide ion or chloride ion. In the crystal structure, molecules are connected through intermolecular dipole interactions of the type N---H...Br and hydrogen bond N---H…O. Additionally, an intramolecular hydrogen bond of the type C---H…Br is observed; these interactions lead to a three dimensional architectural packing in the crystal structure. Hirschfeld surfaces computational method was used to figure out the intercontacts in the crystal structure, the data showed that intercontacts of the type H…H (52.8 %), H…Br (32.7 %), H…O (12.4 %) and Br…O (2.1 %) were

observed and quantified. Antitumor activity of the desired complexes was evaluated. The results revealed high antitumor activity against several types of cancer cells.

Chapter One

Introduction

1.1 The aim

The aims of this study were:

- Four Cu (II) complexes were prepared: five coordinated monocationic-monohydrated-halo-Bis-propane-1,3-diamine/Copper(II) halide complexes.
- The desired complexes were characterized by several available spectral analysis techniques like: IR, UV-Visible, TG/DTA, EA, MS, CV, EDX, and SEM**.**
- X-ray Single crystals diffraction was investigated to identify the structural formulas of crystalline complexes **2** and **4**
- ComputationalHirschfeld surface analysis ofcomplexes **2** and **4** were carried out, in order to compare both theoretical and experimental spectral analysis.
- The complexes were evaluated as DNA-binder as well as antitumoractivities**.**

1.2. Organometallic Chemistry:

Organometallic compounds, with their metal–carbon bonds, are placed at the interface between classical organic and inorganic chemistry in dealing with the interaction between inorganic metal species and organic molecules [1-3]. The organometallic field has provided a series of important conceptual insights, surprising structures, and useful catalysts both for industrial processes and for organic synthesis. Many catalysts are capable of very high levels of asymmetric induction in preferentially forming one

enantiomer of a chiral product. The field is a beginning to make links with biochemistry with the discovery of enzymes that carry out organometallic catalysis [3-4]. Ideas drawn from organometallic chemistry have helped to interpret the chemistry of metal and metal oxide surfaces, both key actors in heterogeneous catalysis. The field is also creating links with the chemistry of materials because organometallic and metal–organic compounds are increasingly preferred as the precursors for depositing materials on various substrates via thermal decomposition of the metal compound. Nanoscience and nanotechnology are also benefiting with the use of such compounds as the most common precursors for nanoparticles. These small particles of a metal or alloy, with properties quite unlike the bulk material, are finding more and more useful applications in electronic, magnetic, or optical devices or in sensors [1-10].

Public concern for the environment has led to the rise of *green chemistry*, with the object of minimizing both energy use and chemical waste in industryand commerce. One strategy is *atom economy* in which reactions are chosen that minimize the formation of by-products or unreacted starting materials.

For example, rhodium or iridium-based catalysts directly convert MeOH and CO to MeCOOH with no significant by products. Organometallic catalysis is likely to be a key contributor when climate change becomes severe enough to force government action to mandate the use of renewable fuels [4-6]. The presence of d electrons in their valence shell distinguishes the organometallic chemistry of the elements of groups 3–12 of the

Periodic Table, the transition elements, from that of groups 1–2 and 12–18, the main-group elements. Group 12, and to some extent also group 3, often show greater resemblance to the main-group elements. Transition metal ions can bind *ligands* (L) to give a coordination compound, or *complex* MLn, as in the familiar aqua ions $[M(OH_2)_6]^{2+}$ (M = V, Cr,Mn, Fe,Co, or Ni). Organometallic chemistry is a subfield of coordination chemistry in which the complex contains an M−CorM−H bond. Organometallic species tend to be more covalent, and the metal is often more reduced, than in other coordination compounds. Typical ligands that usually bind to metals in their lower oxidation states are CO, alkenes, and arenes.. In this chapter we review some fundamental ideas of coordination chemistry, which also apply to organometallic complexes [1-15].

1.3 Stereochemistry:

The most common type of complex is ML_6, which adopts an octahedral coordination geometry (**1.1**) based on one of the Pythagorean regular solids.

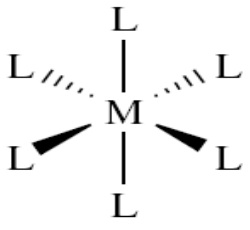

1.1

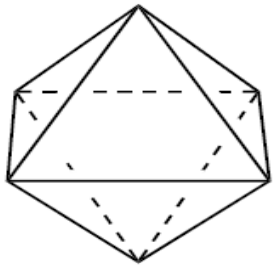

Octahedron

1.4 Chelate Effect

Other ligands can have more than one donor atom, each with its lone pair; an example is ethylenediamine (H_2N-CH_2CH_2-NH_2), often abbreviated "en"). Such ligands most commonly donate both lone pairs to the same metal to give a ring compound, known as a *chelate*, from the Greek word for "claw" (**1.2**). Chelate ligands may be bidentate, such as ethylenediamine, or polydentate, such as **1.3** and **1.4**

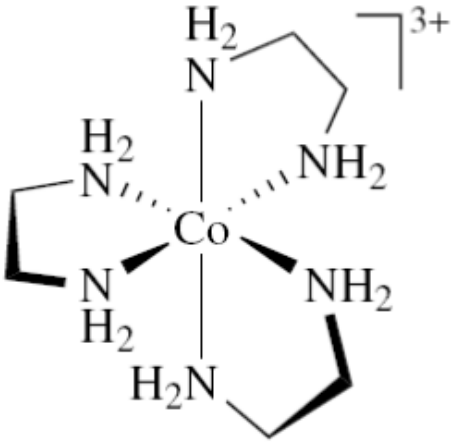

1.2

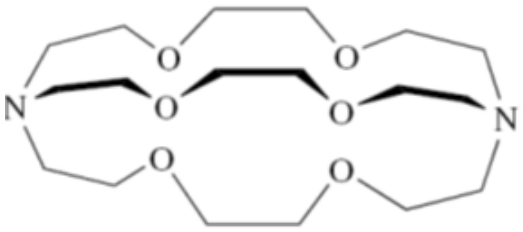

1.3

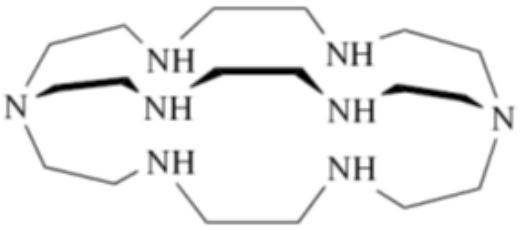

1.4

1.5 Why Copper?

Copper, a bio-essential element, plays an important role in biological processes that involve electron transfer reactions.Actually,copper(II)

complexes with O, N, S have been widely studied and they are proved to be good anticancer agents due to their strong binding affinity with DNA [2-14]. It has been demonstrated that copper assembles in tumors due to the selective permeability of cancer cell membranes to copper compounds [2-11].

It is a very impoal in life, photosynthesis process, mitochondrial respiratory, carbon and nitrogen rtant met metabolism, and oxidative stress protection [14].

1.6. Previous Work

The interaction and reactions of metal complexes with DNA have long been thesubject of intense investigation in relation to the development of new reagents for bio- technology and medicine. Among the metal complexes so far investigated, those of phenanthroline that have attracted much attention for their various functions. It is well known that copper(II) complexes of 1,10-phenanthroline (phen) inhibit DNA or RNA polymerase activities and induce strand scission of DNA in the presence of OH^-or thiol [5-11]. The copper–phenanthroline complex cycles between Cu(II) and Cu(I) to catalyze the formation of activated oxygen species. In the course of such reactions, a tetrahedral [Cu(phen)] complex has been suggested to bind non-intercalatively in the minor groove of the DNA.The substituents on the phenanthroline ring influence the reactivity of the complexes with DNA [5-7]. For example, the copper(I) complex of 2,9-dimethyl-1,10-phenanthro line, [Cu(2,9-dmp)] , does not cleave DNA [5]. It has been also

reported that some ternary complexes of $[Cu(phen)]^{+2}$ have an antitumor activity [13].

Tris-phenanthroline metal complexes and their analogs have also attracted much attention for the chiral recognition of DNA double helices with the enantiomeric complexes and for the photochemical electron-transfer reactions initiated by the complex bound to DNA [3-13].In the case of $[Ru(phen)]^{+2}$, both an intercalative and non-intercalative binding modes have been proposed.

Although various binding structures have been proposedforthe phenanthroline complexes on DNA, the geometrical part that DNA-fiber electron paramagnetic resonance (EPR) ameters, that characterize the binding mode of the complexes, have scarcely been reported. We have shown that spectroscopy provides information on stereospecificity and dynamic principal axes of the *g*-tensors relative to the DNA-double properties of paramagnetic metal complexes bound to DNA [4,16-48]. One can estimate the angles of the helical axis from the changes in the EPR line shapes with the orientation of the DNA fibers in the magnetic field. The temperature dependent EPR line shapes give information on the motion of the complexes on DNA.

1.7 Novelty

1. Water soluble octahedral diaminecopper(II) complexes were prepared for the first time.

2. Novel 3D structure of such Copper-ligands coordinate were analyzed by XRD and compared by DFT optimized structures.
3. The antitumor activity of such complexes was developed depending on their structures.

Chapter Two

Experimental part

2.1 Chemicals

2.1.1 Solvents

Table 2.1: Solvent'sName and Molecular Formula

Solvent name	Chemical Formula	Molar Mass
1. Dichloromethane	CH_2Cl_2	84.93g/mol
2. Hexane	C_6H_{14}	86.17 g/mol
3. Ethanol	CH_3CH_2OH	46.07 g/mol
4. Distilled water	H_2O	18 g/mol
5.Tetrachloromethane	CCl_4	153.81 g/mol

2.1.2 Starting Materials

Other Reagent

Table 2.2 :Starting Material's Name, Molecular Formula and Molar Mass

Chemical Material Name	**Molecular Formula**	**Molar Mass (gram/mole)**	**Physical State at Room Temp.**
Copper(II) Bromide Tetrahydrate	$CuBr_2.4H_2O$	295.41 g/mol	Solid
Cu(II) ChlorideDihydrate	$CuCl_2.2H_2O$	170.48g/mole.	Solid
Propane-1,3-diamine	$C_3H_{10}N_2$	74.13 g/mol	Liquid
1 ,10 Phenanthroline	$C_{12}H_8N_2$	180.21 g/mol	Solid
2,2'-Bipyridine	$C_{10}H_8N_2$	156.19 g / mol	Solid

2.2 Equipments

1. X-Ray Diffractometer (Mysore University, India) was used to determine the structure of crystalline compounds.
2. Perkin Elmer Spectrum 1000 FT-IR Spectrophotometer (An-Najah National University, Palestine) wasused to obtain the spectra of resulting ligands L_1, L_2 and their complexes 1-4.

3. TU-1901 Double-Beam UV–Visible Spectrophotometer (An-Najah National University, Palestine) was used to obtain the maximum wavelength for $L_1$and their complexes 1,2.
4. NMR BrukerAvance II 400 Spectrometer at 298 K, with 5 mm PABBO BB-1H TUBES, using $CDCl_3$ as a Solvent and TMS as Internal Standard (chemical shift in δ ppm) (Mysore University, India) was used to obtain NMR spectra of resulting ligands L_1, L_2
5. TGA-7 PerkinElmer Thermogravimetric Analyzer (PerkinElmer Inc., Waltham, MA, USA) (Mysore University, India) was used to obtain TG/DTG for L_1, L_2, and their complexes 1, 4.
6. Thin-Layer Chromatography using Merck Silica Gel 60 F254 Coated Aluminum Plates (Mysore University, India) was used to determine the purity of the ligands L_1, L_2.
7. EI-MS (Mysore University, India) was used to obtain the spectrum for L_1.

2.3 Synthesis

Procedure to prepare the desired complexes

Complexes **1-4** were synthesized, in 80-90% yields. The corresponding hydrated CuX_2 salt (1 mmol) was dissolved in ethanol (10 mL).To this solution,2mmol of propane-1,3-diamine or ethylenediamine dissolved in distilled water (1 mL) were added. The reaction mixture was left for ~ 10 min until appearance of deep blue color solution. Solvent was then evaporated under reduced pressure and the solid

residue was washed several times with alcohol and dichloromethane and then was left to dry.

Complex **1**

Yield 83%, m.p. = 165 °C. MS (m/z) 246.07 [M+]-Cl for $[C_6H_{20}ClCuN_4]Cl$. Calculated: C, 25.49; H, 7.13; N, 19.82. Found C, 25.34; H, 7.15; N, 19.71%, (IR, νcm^{-1}): 3375-3135 (ν_{H-N}), 2925 (ν_{C-H}), 1555 (ν_{N-H}), 1175 (ν_{N-C}), 515 (ν_{Cu-N}). UV–Vis. in water: $\lambda_{max(}\varepsilon_{max}/M^{-1}$ cm^{-1}): 250 nm (1.25 x 10^3 $M^{-1}L^{-1}$) and 580 nm (3.10 x 10^2 $M^{-1}L^{-1}$).

Complex **2**

Yield 90%, m.p. = 185 °C. MS (m/z) 292.2 [M+]-Br for $[C_6H_{20}BrCuN_4]Br$. Calculated: C, 19.39; H, 5.42; N, 15.08. Found: C, 19.15; H, 5.21; N, 14.92%. (IR, νcm^{-1}): 3380-3250 and 3160 (ν_{H-N}), 2890 (ν_{C-H}), 1565 (ν_{N-H}), 1170 (ν_{N-C}), 508 (ν_{Cu-N}). UV–Vis. in water: $\lambda_{max(}\varepsilon_{max}/M^{-1}$ cm^{-1}): 255 nm (1.20 x 10^3 $M^{-1}L^{-1}$) and 568 nm (2.90 x 10^2 $M^{-1}L^{-1}$).

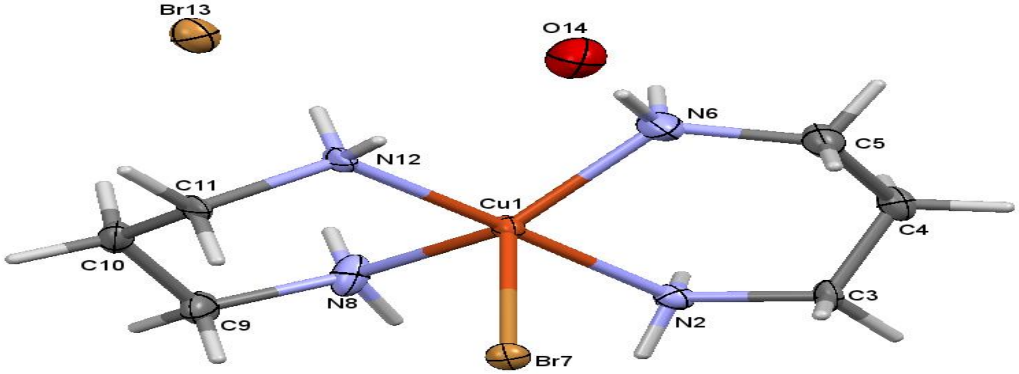

Complex **3**

Yield 78%, m.p. = 178 °C. MS (m/z) 219[M+]-Cl for $[C_4H_{16}ClCuN_4]Cl$. Calculated: C, 25.49; H, 7.13; N, 19.82. Found C, 25.34; H, 7.15; N, 19.71%, (IR, νcm^{-1}): 3375-3135 (ν_{H-N}), 2925 (ν_{C-H}), 1555 (ν_{N-H}), 1175 (ν_{N-C}), 515 (ν_{Cu-N}). UV–Vis. in water: λ_{max}(ε_{max}/M^{-1} cm^{-1}): 250 nm (1.25 x 10^3 M^{-1}L^{-1}) and 580 nm (3.10 x 10^2 M^{-1}L^{-1}).

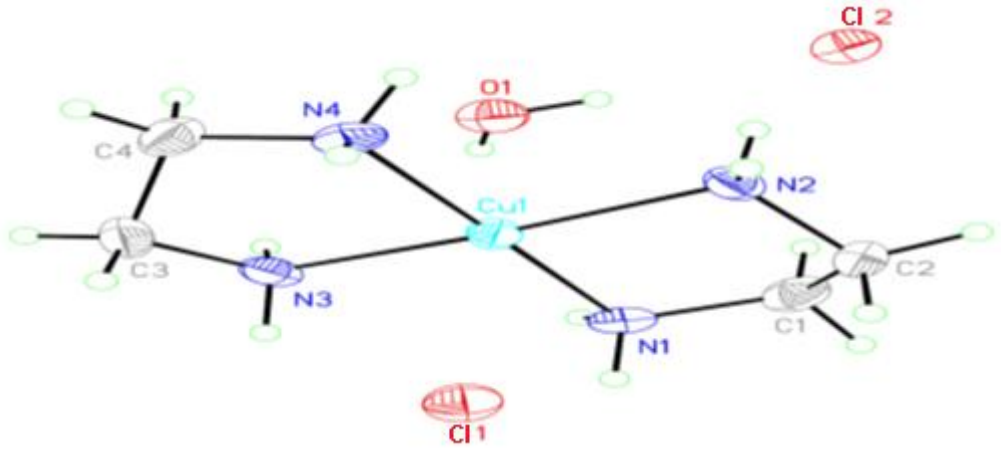

Complex **4**

Yield 90%, m.p. = 185 °C. MS (m/z) 263 [M+]-Br for $[C_4H_{16}BrCuN_4]Br$. Calculated: C, 19.39; H, 5.42; N, 15.08. Found: C, 19.15; H, 5.21; N, 14.92%. (IR, νcm^{-1}): 3380-3250 and 3160 (ν_{H-N}), 2890 (ν_{C-H}), 1565 (ν_{N-H}), 1170 (ν_{N-C}), 508 (ν_{Cu-N}). UV–Vis.in water: λ_{max}(ε_{max}/M^{-1} cm^{-1}): 255 nm (1.20 x 10^3 M^{-1}L^{-1}) and 568nm (2.90 x 10^2 M^{-1}L^{-1}).

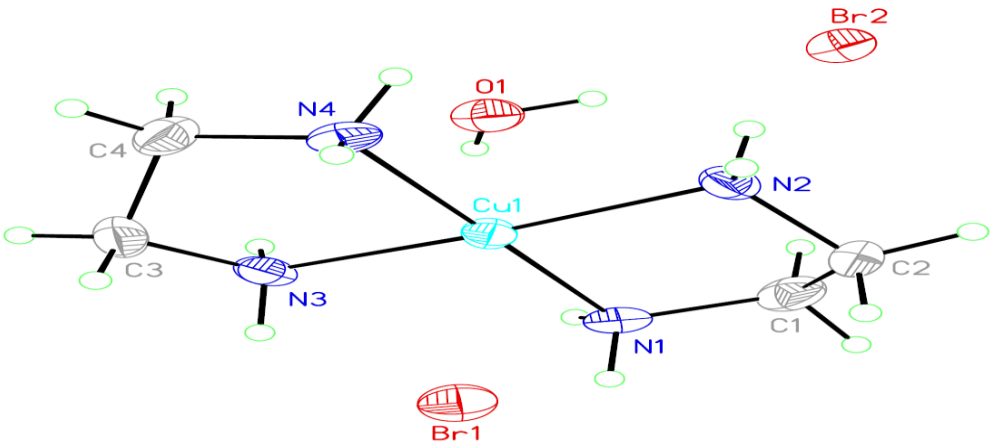

2.4 Instruments

A TU-1901 double-beam UV–visible spectrophotometer was employed to record the UV-visible spectra for complexes, whereas Infrared spectra (IR) were recorded on a Perkin Elmer Spectrum 1000 FT-IR Spectrophotometer. EI-MS data were obtained with the aid of a Finnigan 711A (8 kV) (PerkinElmer Inc., Waltham, MA, USA) instrument. Thermogravimetric analysis (TGA) and differential thermal analysis (DTA) for both complexes were accomplished by using a TGA-7 Perkin Elmer thermogravimetric analyzer (Perkin Elmer Inc., Waltham, MA, USA). Elemental analysis (C, H, and N) for complex 2 was performed out with EuroVector EA3000 (C, H, and N) instrument, and the observed results agreed with the calculated percentages to within ± 0.4%. We carried out Hirshfeld surface analysis for complex **2** using the program CRYSTAL EXPLORER 3.1 [34].

2.4.1 Single Crystal X-ray Diffraction

By a slow evaporation of ethanol from ethanolic solution of the complex, suitable crystal for X-ray diffraction measurements was collected. A blue-prism single crystal of dimensions 0.27×0.28×0.26 mm of complex **2** was selected for X-ray diffraction measurements. X-ray intensity data were collected at a temperature of 293 K with the aid of a BrukerProteum 2 CCD diffractometer equipped with an X-ray generator operating at 45 kV and 10 mA, using CuK_{α} radiation of wavelength 1.54178Å. Data was collected for 24 frames per set with different settings of φ(0° and 90°), keeping a scan

width of 0.5°, exposure time of 2 s, sample to detector distance of 45.10 mm and 2θvalue at 64.5°. A complete data set was processed using *SAINT PLUS* [35]. Crystal structure was solved by direct methods and refined with full-matrix least squares method by means of the F^2 *SHELXS* and *SHELXL* programs [36]. Geometrical calculations were carried out using the program *PLATON* [37], whereasthe molecular and packing diagrams were generated with the aid of the software *MERCURY* [38]. Details of the crystal structure and data refinement are given in **Table 2.3**.

Table 2.3 Crystallographic data and structure refinement parameters for complex 2.

Empirical formula	**$C_6H_{22}N_4Br_2OCu$**
Formula weight	389.61
Temperature	293(2) K
Wavelength	1.54178 Å
Crystal system, space group	Monoclinic, $P2_1/c$
Unit cell dimensions	a = 8.6858(5) Å
Volume	1326.95(13) $Å^3$
Z, Calculated density	4, 1.940 Mg/m^3
Absorption coefficient	9.230 mm^{-1}
$F_{(000)}$	764
Crystal size	0.26 x 0.27 x 0.28 mm
Theta range for data collection	5.3° to 64.5°
Limiting indices	$-7 \leq h \leq 10$, $-17 \leq k \leq 15$, $-12 \leq l \leq$
Reflections collected / unique	5668/ 2107 [R(int) = 0.039]
Refinement method	Full-matrix least-squares on F^2
Data / restraints / parameters	2021 / 0 / 128
Goodness-of-fit on F^2	1.11
Largest diff. peak and hole	1.22 And −0.90e. $Å^{-3}$

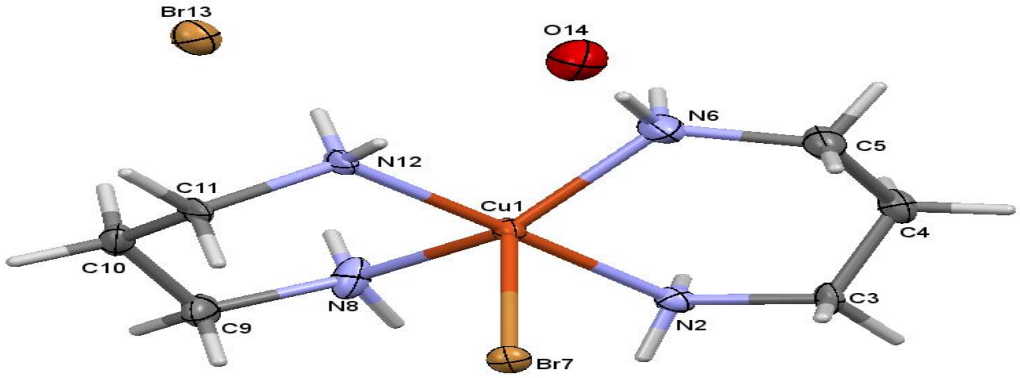

Table 2.4: Bond lengths Å and angles (°) for complex 2

Cu1—N2	2.011 (4)	N6—H6A	0.9000
Cu1—N12	2.020 (4)	N6—H6B	0.9000
Cu1—N8	2.051 (4)	N8—C9	1.489 (6)
Cu1—N6	2.053 (4)	N8—H8A	0.9000
Cu1—Br7	2.7089 (7)	N8—H8B	0.9000
N2—C3	1.478 (6)	C9—C10	1.499 (6)
N2—H2A	0.9000	C9—H9A	0.9700
N2—H2B	0.9000	C9—H9B	0.9700
C3—C4	1.512 (6)	C10—C11	1.511 (6)
C3—H3A	0.9700	C10—H10A	0.9700
C3—H3B	0.9700	C10—H10B	0.9700
C4—C5	1.517 (6)	C11—N12	1.487 (5)
C4—H4A	0.9700	C11—H11A	0.9700
C4—H4B	0.9700	C11—H11B	0.9700
C5—N6	1.465 (7)	N12—H12A	0.9000
C5—H5A	0.9700	N12—H12B	0.9000
C5—H5B	0.9700		
N2—Cu1—N12	179.01 (13)	C5—N6—H6A	106.6
N2—Cu1—N8	89.50 (15)	Cu1—N6—H6A	106.6
N12—Cu1—N8	90.18 (15)	C5—N6—H6B	106.6
N2—Cu1—N6	90.30 (15)	Cu1—N6—H6B	106.6
N12—Cu1—N6	90.52 (15)	H6A—N6—H6B	106.6
N8—Cu1—N6	143.54 (17)	C9—N8—Cu1	118.3 (3)
N2—Cu1—Br7	87.27 (9)	C9—N8—H8A	107.7
N12—Cu1—Br7	91.89 (10)	Cu1—N8—H8A	107.7
N8—Cu1—Br7	101.87 (11)	C9—N8—H8B	107.7
N6—Cu1—Br7	114.54 (13)	Cu1—N8—H8B	107.7
C3—N2—Cu1	116.8 (3)	H8A—N8—H8B	107.1
C3—N2—H2A	108.1	N8—C9—C10	111.7 (4)
Cu1—N2—H2A	108.1	N8—C9—H9A	109.3
C3—N2—H2B	108.1	C10—C9—H9A	109.3
Cu1—N2—H2B	108.1	N8—C9—H9B	109.3
H2A—N2—H2B	107.3	C10—C9—H9B	109.3

N2—C3—C4	110.9 (4)	H9A—C9—H9B	107.9
N2—C3—H3A	109.5	C9—C10—C11	114.3 (4)
C4—C3—H3A	109.5	C9—C10—H10A	108.7
N2—C3—H3B	109.5	C11—C10—H10A	108.7
C4—C3—H3B	109.5	C9—C10—H10B	108.7
H3A—C3—H3B	108.1	C11—C10—H10B	108.7
C3—C4—C5	112.4 (4)	H10A—C10—H10B	107.6
C3—C4—H4A	109.1	N12—C11—C10	112.3 (3)
C5—C4—H4A	109.1	N12—C11—H11A	109.1
C3—C4—H4B	109.1	C10—C11—H11A	109.1
C5—C4—H4B	109.1	N12—C11—H11B	109.1
H4A—C4—H4B	107.9	C10—C11—H11B	109.1
N6—C5—C4	112.0 (4)	H11A—C11—H11B	107.9
N6—C5—H5A	109.2	C11—N12—Cu1	116.6 (3)
C4—C5—H5A	109.2	C11—N12—H12A	108.1
N6—C5—H5B	109.2	Cu1—N12—H12A	108.1
C4—C5—H5B	109.2	C11—N12—H12B	108.1
H5A—C5—H5B	107.9	Cu1—N12—H12B	108.1
C5—N6—Cu1	122.8 (3)	H12A—N12—H12B	107.3

Table 2.5:Atomic displacement parameters (Å^2)

	U^{11}	U^{22}	U^{33}	U^{12}	U^{13}	U^{23}
Cu1	0.0085 (5)	0.0138 (4)	0.0168 (4)	−0.0003 (2)	0.0040 (3)	−0.0014 (2)
N2	0.0134 (19)	0.0140 (16)	0.0171 (17)	0.0001 (14)	0.0068 (15)	0.0005 (13)
C3	0.007 (2)	0.021 (2)	0.019 (2)	−0.0006 (16)	0.0047 (18)	0.0019 (16)
C4	0.012 (2)	0.022 (2)	0.026 (2)	0.0004 (17)	0.008 (2)	0.0035 (17)
C5	0.015 (3)	0.025 (2)	0.034 (3)	0.0032 (19)	0.007 (2)	−0.0006 (19)
N6	0.018 (2)	0.030 (2)	0.039 (3)	0.0026 (17)	0.0076 (19)	−0.0139 (18)
Br7	0.0154 (4)	0.0152 (3)	0.0147 (3)	−0.00021 (15)	0.0069 (2)	0.00247 (14)
N8	0.014 (2)	0.0237 (19)	0.026 (2)	−0.0048 (16)	−0.0003 (17)	0.0080 (15)
C9	0.016 (2)	0.022 (2)	0.024 (2)	0.0060 (18)	−0.0002 (19)	0.0004 (18)
C10	0.011 (2)	0.033 (2)	0.017 (2)	0.0027 (18)	0.0021 (19)	0.0006 (17)
C11	0.007 (2)	0.022 (2)	0.025 (2)	−0.0028 (17)	0.0080 (19)	−0.0073 (18)
N12	0.0075 (19)	0.0205 (17)	0.025 (2)	−0.0011 (14)	0.0072 (16)	−0.0079 (15)
Br1	0.0209 (4)	0.0247 (4)	0.0260 (4)	0.00193 (18)	0.0105 (3)	0.00446 (18)
O14	0.029 (2)	0.047 (2)	0.045 (2)	−0.0008 (18)	0.0075 (19)	−0.0094 (19)

Table 2.6:Fractional atomic coordinates and isotropic or equivalent isotropic displacement parameters (Å^2)

	x	*Y*	*Z*	U_{iso}*/U_{eq}	
Cu1	0.48187 (8)	0.62620 (4)	0.19870 (6)	0.0133 (3)	
N2	0.2878 (4)	0.5477 (2)	0.0956 (3)	0.0145 (7)	
H2A	0.3235	0.5073	0.0521	0.017*	
H2B	0.2564	0.5178	0.1530	0.017*	
C3	0.1389 (6)	0.5923 (3)	−0.0003 (4)	0.0158 (9)	
H3A	0.0593	0.5477	−0.0512	0.019*	
H3B	0.1710	0.6275	−0.0605	0.019*	
C4	0.0580 (6)	0.6519 (3)	0.0687 (5)	0.0200 (10)	
H4A	0.0482	0.6196	0.1416	0.024*	
H4B	−0.0537	0.6671	0.0080	0.024*	
C5	0.1563 (6)	0.7368 (3)	0.1199 (5)	0.0253 (10)	
H5A	0.1693	0.7681	0.0475	0.030*	
H5B	0.0944	0.7750	0.1559	0.030*	
N6	0.3213 (5)	0.7188 (3)	0.2215 (4)	0.0301 (10)	
H6A	0.3049	0.7035	0.2946	0.036*	
H6B	0.3764	0.7710	0.2390	0.036*	
Br7	0.53913 (5)	0.64427 (3)	−0.02482 (4)	0.0148 (2)	
N8	0.6193 (5)	0.5150 (3)	0.2812 (4)	0.0239 (9)	
H8A	0.6217	0.5095	0.3632	0.029*	
H8B	0.5641	0.4674	0.2353	0.029*	
C9	0.7944 (6)	0.5099 (3)	0.2896 (5)	0.0230 (10)	
H9A	0.7942	0.5100	0.2016	0.028*	
H9B	0.8442	0.4545	0.3317	0.028*	
C10	0.8973 (6)	0.5864 (3)	0.3659 (4)	0.0213 (10)	
H10A	1.0127	0.5764	0.3782	0.026*	
H10B	0.8920	0.5876	0.4521	0.026*	
C11	0.8437 (5)	0.6762 (3)	0.3017 (4)	0.0177 (9)	
H11A	0.9269	0.7204	0.3487	0.021*	
H11B	0.8378	0.6737	0.2121	0.021*	
N12	0.6788 (4)	0.7043 (2)	0.3003 (4)	0.0174 (8)	
H12A	0.6574	0.7596	0.2666	0.021*	
H12B	0.6867	0.7073	0.3840	0.021*	
Br13	0.73722 (6)	0.59257 (3)	0.65539 (5)	0.0234 (3)	
O14	0.3373 (5)	0.6142 (3)	0.4568 (4)	0.0423 (10)	

Table 2.7: Torsion angles in complex 2

Number	Atom1	Atom2	Atom3	Atom4	Torsion
1	N6	Cu1	N2	H2A	163.4
2	N6	Cu1	N2	H2B	-80.7
3	N6	Cu1	N2	C3	41.3(3)
4	Br7	Cu1	N2	H2A	48.9
5	Br7	Cu1	N2	H2B	164.8
6	Br7	Cu1	N2	C3	-73.2(3)
7	N8	Cu1	N2	H2A	-53
8	N8	Cu1	N2	H2B	62.9
9	N8	Cu1	N2	C3	-175.1(3)
10	N12	Cu1	N2	H2A	17
11	N12	Cu1	N2	H2B	133
12	N12	Cu1	N2	C3	-105(8)
13	N2	Cu1	N6	C5	-35.2(4)
14	N2	Cu1	N6	H6A	88.1
15	N2	Cu1	N6	H6B	-158.4
16	Br7	Cu1	N6	C5	52.0(4)
17	Br7	Cu1	N6	H6A	175.2
18	Br7	Cu1	N6	H6B	-71.3
19	N8	Cu1	N6	C5	-124.7(4)
20	N8	Cu1	N6	H6A	-1.5
21	N8	Cu1	N6	H6B	112
22	N12	Cu1	N6	C5	144.3(4)
23	N12	Cu1	N6	H6A	-92.5
24	N12	Cu1	N6	H6B	21.1
25	N2	Cu1	N8	H8A	-102.5
26	N2	Cu1	N8	H8B	12.6
27	N2	Cu1	N8	C9	135.0(4)
28	N6	Cu1	N8	H8A	-12.7
29	N6	Cu1	N8	H8B	102.5
30	N6	Cu1	N8	C9	-135.2(4)
31	Br7	Cu1	N8	H8A	170.4
32	Br7	Cu1	N8	H8B	-74.5
33	Br7	Cu1	N8	C9	47.9(4)
34	N12	Cu1	N8	H8A	78.4
35	N12	Cu1	N8	H8B	-166.4
36	N12	Cu1	N8	C9	-44.1(4)
37	N2	Cu1	N12	C11	-25(9)
38	N2	Cu1	N12	H12A	97
39	N2	Cu1	N12	H12B	-147
40	N6	Cu1	N12	C11	-171.3(3)
41	N6	Cu1	N12	H12A	-49.3

42	N6	Cu1	N12	H12B	66.7
43	Br7	Cu1	N12	C11	-56.7(3)
44	Br7	Cu1	N12	H12A	65.3
45	Br7	Cu1	N12	H12B	-178.7
46	N8	Cu1	N12	C11	45.2(3)
47	N8	Cu1	N12	H12A	167.1
48	N8	Cu1	N12	H12B	-76.8
49	Cu1	N2	C3	H3A	173.2
50	Cu1	N2	C3	H3B	55.1
51	Cu1	N2	C3	C4	-65.9(4)
52	H2A	N2	C3	H3A	51.2
53	H2A	N2	C3	H3B	-67
54	H2A	N2	C3	C4	172.1
55	H2B	N2	C3	H3A	-64.7
56	H2B	N2	C3	H3B	177.1
57	H2B	N2	C3	C4	56.1
58	N2	C3	C4	H4A	-46.9
59	N2	C3	C4	H4B	-164.4
60	N2	C3	C4	C5	74.4(5)
61	H3A	C3	C4	H4A	74
62	H3A	C3	C4	H4B	-43.5
63	H3A	C3	C4	C5	-164.8
64	H3B	C3	C4	H4A	-167.8
65	H3B	C3	C4	H4B	74.7
66	H3B	C3	C4	C5	-46.5
67	C3	C4	C5	H5A	56.9
68	C3	C4	C5	H5B	174.8
69	C3	C4	C5	N6	-64.1(5)
70	H4A	C4	C5	H5A	178.1
71	H4A	C4	C5	H5B	-64
72	H4A	C4	C5	N6	57.1
73	H4B	C4	C5	H5A	-64.3
74	H4B	C4	C5	H5B	53.6
75	H4B	C4	C5	N6	174.7
76	C4	C5	N6	Cu1	49.5(5)
77	C4	C5	N6	H6A	-73.7
78	C4	C5	N6	H6B	172.7
79	H5A	C5	N6	Cu1	-71.6
80	H5A	C5	N6	H6A	165.2
81	H5A	C5	N6	H6B	51.7
82	H5B	C5	N6	Cu1	170.5
83	H5B	C5	N6	H6A	47.3
84	H5B	C5	N6	H6B	-66.2

85	Cu1	N8	C9	H9A	-62.9
86	Cu1	N8	C9	H9B	179.1
87	Cu1	N8	C9	C10	58.2(5)
88	H8A	N8	C9	H9A	174.6
89	H8A	N8	C9	H9B	56.7
90	H8A	N8	C9	C10	-64.3
91	H8B	N8	C9	H9A	59.5
92	H8B	N8	C9	H9B	-58.5
93	H8B	N8	C9	C10	-179.5
94	N8	C9	C10	H10A	172.9
95	N8	C9	C10	H10B	56
96	N8	C9	C10	C11	-65.6(5)
97	H9A	C9	C10	H10A	-66.1
98	H9A	C9	C10	H10B	177.1
99	H9A	C9	C10	C11	55.4
100	H9B	C9	C10	H10A	51.9
101	H9B	C9	C10	H10B	-65
102	H9B	C9	C10	C11	173.4
103	C9	C10	C11	H11A	-170.3
104	C9	C10	C11	H11B	-52.6
105	C9	C10	C11	N12	68.6(5)
106	H10A	C10	C11	H11A	-48.8
107	H10A	C10	C11	H11B	68.9
108	H10A	C10	C11	N12	-169.9
109	H10B	C10	C11	H11A	68.1
110	H10B	C10	C11	H11B	-174.3
111	H10B	C10	C11	N12	-53.1
112	C10	C11	N12	Cu1	-62.2(4)
113	C10	C11	N12	H12A	175.8
114	C10	C11	N12	H12B	59.8
115	H11A	C11	N12	Cu1	176.6
116	H11A	C11	N12	H12A	54.6
117	H11A	C11	N12	H12B	-61.4
118	H11B	C11	N12	Cu1	59
119	H11B	C11	N12	H12A	-63
120	H11B	C11	N12	H12B	-179

Table 2.8: Crystal data and structure refinement for complex 4

Empirical formula	**$C_4H_{18}Br_2CuN_4O$**
Formula weight	361.58
Temperature	293(2) K
Wavelength	0.71073 Å
Crystal system	Monoclinic
Space group	P 1 21/n 1
Unit cell dimensions	a = 6.4422(4) Åα= 90° b = 15.4116(9) Åβ= 98.048(6)° c = 12.0398(9) Åγ = 90°
Volume	1183.59(13) $Å^3$
Z	4
Density (calculated)	2.029 Mg/m^3
Absorption coefficient	8.567 mm^{-1}
F(000)	708
Crystal size	0.3 x 0.2 x 0.2 mm^3
The range of data collection	3.15 to 26.30°
Index ranges	-8<=h<=7,-19<=k<=17, -12<=l<=15
Reflections collected	5508
Independent reflections	2385 [R(int) = 0.0394]
Completeness to theta = 26.30°	99.9%
Absorption correction	Semi-empirical from equivalents
Max. and min. transmission	1.00000 and 0.42392
Refinement method	Full-matrix least-squares on F^2
Data / restraints / parameters	2385 / 1 / 115
Goodness-of-fit on F^2	0.989
Final R indices [I>2sigma(I)]	R1 = 0.0422, wR2 = 0.0595
R indices (all data)	R1 = 0.0675, wR2 = 0.0661
Largest diff. peak and hole	0.683 and -0.649 $e.Å^{-3}$

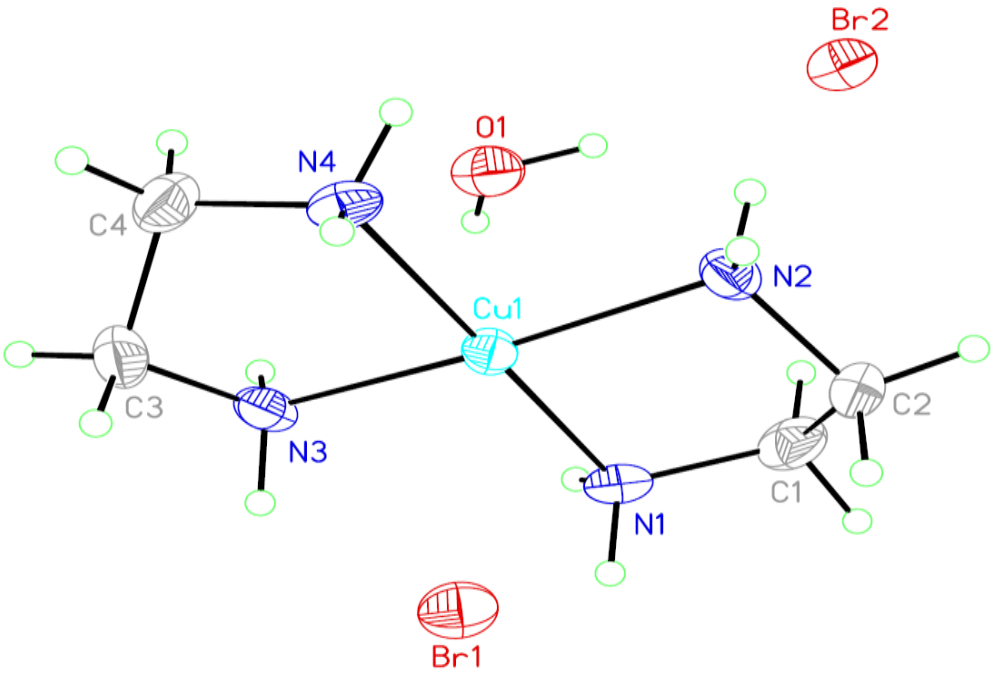

Table 2.9: Atomic coordinates (x 10^4) and equivalent isotropic displacement parameters ($Å^2$x 10^3) complex 4.

	x	y	z	U(eq)
Br(1)	1619(1)	2962(1)	5440(1)	43(1)
Cu(1)	-2556(1)	2723(1)	4123(1)	33(1)
Br(2)	-7531(1)	625(1)	2476(1)	55(1)
N(4)	-1700(6)	3296(2)	2772(3)	39(1)
N(3)	-3323(6)	3934(2)	4551(3)	41(1)
C(4)	-2496(8)	4190(3)	2704(4)	54(2)
C(3)	-2311(9)	4548(3)	3872(4)	55(2)
N(1)	-3426(6)	2159(2)	5483(3)	38(1)
O(1)	-6558(6)	2657(2)	3051(3)	59(1)
N(2)	-2122(6)	1493(2)	3614(3)	39(1)
C(2)	-1992(8)	927(3)	4621(4)	49(1)
C(1)	-3660(8)	1219(3)	5298(4)	53(2)

Table 2.10: Bond lengths Å and angles ° for complex 4

Bond	Length (Å)
Cu(1)-N(4)	1.996(3)
Cu(1)-N(1)	2.002(3)
Cu(1)-N(3)	2.017(3)
Cu(1)-N(2)	2.023(3)
N(4)-C(4)	1.468(5)
N(4)-H(4A)	0.9
N(4)-H(4D)	0.9
N(3)-C(3)	1.463(5)
N(3)-H(3A)	0.9
N(3)-H(3D)	0.9
C(4)-C(3)	1.500(6)
C(4)-H(4B)	0.97
C(4)-H(4C)	0.97
C(3)-H(3B)	0.97
C(3)-H(3C)	0.97
N(1)-C(1)	1.471(5)
N(1)-H(1A)	0.9
N(1)-H(1D)	0.9
O(1)-H(1)	0.93(4)
O(1)-H(2)	0.77(5)
N(2)-C(2)	1.487(5)
N(2)-H(2A)	0.9
N(2)-H(2D)	0.9
C(2)-C(1)	1.505(6)
C(2)-H(2B)	0.97
C(2)-H(2C)	0.97
C(1)-H(1B)	0.97
C(1)-H(1C)	0.97
N(4)-Cu(1)-N(1)	179.43(15)
N(4)-Cu(1)-N(3)	84.51(15)
N(1)-Cu(1)-N(3)	94.92(15)
N(4)-Cu(1)-N(2)	95.87(15)

N(1)-Cu(1)-N(2)	84.69(15)
N(3)-Cu(1)-N(2)	173.64(15)
C(4)-N(4)-Cu(1)	109.0(3)
C(4)-N(4)-H(4A)	109.9
Cu(1)-N(4)-H(4A)	109.9
C(4)-N(4)-H(4D)	109.9
Cu(1)-N(4)-H(4D)	109.9
H(4A)-N(4)-H(4D)	108.3
C(3)-N(3)-Cu(1)	108.1(3)
C(3)-N(3)-H(3A)	110.1
Cu(1)-N(3)-H(3A)	110.1
C(3)-N(3)-H(3D)	110.1
Cu(1)-N(3)-H(3D)	110.1
H(3A)-N(3)-H(3D)	108.4
N(4)-C(4)-C(3)	108.2(4)
N(4)-C(4)-H(4B)	110.1
C(3)-C(4)-H(4B)	110.1
N(4)-C(4)-H(4C)	110.1
C(3)-C(4)-H(4C)	110.1
H(4B)-C(4)-H(4C)	108.4
N(3)-C(3)-C(4)	107.6(4)
N(3)-C(3)-H(3B)	110.2
C(4)-C(3)-H(3B)	110.2
N(3)-C(3)-H(3C)	110.2
C(4)-C(3)-H(3C)	110.2
H(3B)-C(3)-H(3C)	108.5
C(1)-N(1)-Cu(1)	109.8(2)
C(1)-N(1)-H(1A)	109.7
Cu(1)-N(1)-H(1A)	109.7
C(1)-N(1)-H(1D)	109.7
Cu(1)-N(1)-H(1D)	109.7
H(1A)-N(1)-H(1D)	108.2
H(1)-O(1)-H(2)	108(4)
C(2)-N(2)-Cu(1)	107.3(3)

C(2)-N(2)-H(2A)	110.2
Cu(1)-N(2)-H(2A)	110.2
C(2)-N(2)-H(2D)	110.2
Cu(1)-N(2)-H(2D)	110.2
H(2A)-N(2)-H(2D)	108.5
N(2)-C(2)-C(1)	107.6(4)
N(2)-C(2)-H(2B)	110.2
C(1)-C(2)-H(2B)	110.2
N(2)-C(2)-H(2C)	110.2
C(1)-C(2)-H(2C)	110.2
H(2B)-C(2)-H(2C)	108.5
N(1)-C(1)-C(2)	108.1(4)
N(1)-C(1)-H(1B)	110.1
C(2)-C(1)-H(1B)	110.1
N(1)-C(1)-H(1C)	110.1
C(2)-C(1)-H(1C)	110.1
H(1B)-C(1)-H(1C)	108.4

Table 2.11: Torsion angles of complex 4

Number	Atom1	Atom2	Atom3	Atom4	Torsion
1	Br1	Cu1	N4	H4A	19.3
2	Br1	Cu1	N4	H4D	138.3
3	Br1	Cu1	N4	C4	-101.1(3)
4	N3	Cu1	N4	H4A	108.2
5	N3	Cu1	N4	H4D	-132.8
6	N3	Cu1	N4	C4	-12.3(3)
7	N1	Cu1	N4	H4A	113
8	N1	Cu1	N4	H4D	-128
9	N1	Cu1	N4	C4	-8(15)
10	O1	Cu1	N4	H4A	-167.1
11	O1	Cu1	N4	H4D	-48.1
12	O1	Cu1	N4	C4	72.4(3)
13	N2	Cu1	N4	H4A	-78.2
14	N2	Cu1	N4	H4D	40.8
15	N2	Cu1	N4	C4	161.3(3)
16	Br1	Cu1	N3	H3A	-163.1
17	Br1	Cu1	N3	H3D	-43.6

18	Br1	Cu1	N3	C3	76.6(3)
19	N4	Cu1	N3	H3A	104.1
20	N4	Cu1	N3	H3D	-136.4
21	N4	Cu1	N3	C3	-16.2(3)
22	N1	Cu1	N3	H3A	-75.9
23	N1	Cu1	N3	H3D	43.6
24	N1	Cu1	N3	C3	163.8(3)
25	O1	Cu1	N3	H3A	14.6
26	O1	Cu1	N3	H3D	134.1
27	O1	Cu1	N3	C3	-105.7(3)
28	N2	Cu1	N3	H3A	10
29	N2	Cu1	N3	H3D	130
30	N2	Cu1	N3	C3	-110(1)
31	Br1	Cu1	N1	H1A	12.9
32	Br1	Cu1	N1	H1D	131.6
33	Br1	Cu1	N1	C1	-107.8(3)
34	N4	Cu1	N1	H1A	-81
35	N4	Cu1	N1	H1D	38
36	N4	Cu1	N1	C1	159(15)
37	N3	Cu1	N1	H1A	-76
38	N3	Cu1	N1	H1D	42.7
39	N3	Cu1	N1	C1	163.3(3)
40	O1	Cu1	N1	H1A	-160.6
41	O1	Cu1	N1	H1D	-42
42	O1	Cu1	N1	C1	78.7(3)
43	N2	Cu1	N1	H1A	110.4
44	N2	Cu1	N1	H1D	-130.9
45	N2	Cu1	N1	C1	-10.3(3)
46	Br1	Cu1	O1	H1	-145(3)
47	Br1	Cu1	O1	H2	-34(4)
48	N4	Cu1	O1	H1	110(3)
49	N4	Cu1	O1	H2	-139(4)
50	N3	Cu1	O1	H1	-165(3)
51	N3	Cu1	O1	H2	-54(4)
52	N1	Cu1	O1	H1	-71(3)
53	N1	Cu1	O1	H2	41(4)
54	N2	Cu1	O1	H1	14(3)
55	N2	Cu1	O1	H2	125(4)
56	Br1	Cu1	N2	H2A	-171.3
57	Br1	Cu1	N2	H2D	-51.5

58	Br1	Cu1	N2	C2	68.6(3)
59	N4	Cu1	N2	H2A	-77.8
60	N4	Cu1	N2	H2D	42
61	N4	Cu1	N2	C2	162.1(3)
62	N3	Cu1	N2	H2A	15
63	N3	Cu1	N2	H2D	135
64	N3	Cu1	N2	C2	-105(1)
65	N1	Cu1	N2	H2A	102.1
66	N1	Cu1	N2	H2D	-138.1
67	N1	Cu1	N2	C2	-18.0(3)
68	O1	Cu1	N2	H2A	11
69	O1	Cu1	N2	H2D	130.8
70	O1	Cu1	N2	C2	-109.0(3)
71	Cu1	N4	C4	H4B	-82.3
72	Cu1	N4	C4	H4C	158.3
73	Cu1	N4	C4	C3	37.9(4)
74	H4A	N4	C4	H4B	157.2
75	H4A	N4	C4	H4C	37.7
76	H4A	N4	C4	C3	-82.6
77	H4D	N4	C4	H4B	38.2
78	H4D	N4	C4	H4C	-81.2
79	H4D	N4	C4	C3	158.4
80	Cu1	N3	C3	C4	40.9(4)
81	Cu1	N3	C3	H3B	-79.3
82	Cu1	N3	C3	H3C	161.1
83	H3A	N3	C3	C4	-79.4
84	H3A	N3	C3	H3B	160.4
85	H3A	N3	C3	H3C	40.8
86	H3D	N3	C3	C4	161.2
87	H3D	N3	C3	H3B	41
88	H3D	N3	C3	H3C	-78.6
89	N4	C4	C3	N3	-52.3(5)
90	N4	C4	C3	H3B	67.9
91	N4	C4	C3	H3C	-172.6
92	H4B	C4	C3	N3	67.9
93	H4B	C4	C3	H3B	-171.9
94	H4B	C4	C3	H3C	-52.3
95	H4C	C4	C3	N3	-172.7
96	H4C	C4	C3	H3B	-52.5
97	H4C	C4	C3	H3C	67.1

98	Cu1	N1	C1	C2	36.3(4)
99	Cu1	N1	C1	H1B	-84
100	Cu1	N1	C1	H1C	156.6
101	H1A	N1	C1	C2	-84.3
102	H1A	N1	C1	H1B	155.4
103	H1A	N1	C1	H1C	36
104	H1D	N1	C1	C2	156.9
105	H1D	N1	C1	H1B	36.7
106	H1D	N1	C1	H1C	-82.8
107	Cu1	N2	C2	H2B	-78
108	Cu1	N2	C2	H2C	162.4
109	Cu1	N2	C2	C1	42.3(4)
110	H2A	N2	C2	H2B	162
111	H2A	N2	C2	H2C	42.4
112	H2A	N2	C2	C1	-77.8
113	H2D	N2	C2	H2B	42.1
114	H2D	N2	C2	H2C	-77.6
115	H2D	N2	C2	C1	162.3
116	N2	C2	C1	N1	-52.1(5)
117	N2	C2	C1	H1B	68.2
118	N2	C2	C1	H1C	-172.5
119	H2B	C2	C1	N1	68.2
120	H2B	C2	C1	H1B	-171.5
121	H2B	C2	C1	H1C	-52.2
122	H2C	C2	C1	N1	-172.3
123	H2C	C2	C1	H1B	-51.9
124	H2C	C2	C1	H1C	67.4

Table 2.12: Anisotropic displacement parameters ($Å^2$ x10^3) for complex 4

	U11	U22	U33	U23	U13	U12
Br(1)	30(1)	55(1)	44(1)	1(1)	-1(1)	4(1)
Cu(1)	37(1)	32(1)	30(1)	-2(1)	9(1)	2(1)
Br(2)	53(1)	64(1)	47(1)	8(1)	5(1)	-3(1)
N(4)	30(2)	56(3)	31(2)	5(2)	2(2)	-1(2)
N(3)	42(3)	42(2)	37(2)	-12(2)	-4(2)	3(2)
C(4)	59(4)	48(3)	51(4)	16(3)	-5(3)	1(3)
C(3)	68(4)	30(3)	64(4)	0(3)	-6(3)	-2(3)
N(1)	32(2)	56(3)	25(2)	1(2)	1(2)	2(2)
O(1)	62(3)	69(3)	45(3)	1(2)	5(2)	-3(2)
N(2)	42(3)	37(2)	38(3)	-8(2)	4(2)	3(2)
C(2)	62(4)	33(3)	48(3)	5(2)	-6(3)	5(3)
C(1)	59(4)	57(4)	41(3)	17(3)	7(3)	-8(3)

Table 2.13: Hydrogen coordinates (x 10^4) and isotropic displacement parameters ($Å^2$x 10^3)for complex 4.

	x	y	z	U(eq)
H(4A)	-293	3299	2820	47
H(4D)	-2224	3001	2150	47
H(3A)	-4723	4004	4425	49
H(3D)	-2884	4027	5285	49
H(4B)	-3950	4197	2359	65
H(4C)	-1687	4541	2251	65
H(3B)	-846	4619	4179	66
H(3C)	-2991	5110	3866	66
H(1A)	-2454	2261	6082	46
H(1D)	-4651	2386	5623	46
H(2A)	-3200	1329	3100	47
H(2D)	-932	1457	3305	47
H(2B)	-618	975	5064	59
H(2C)	-2219	326	4397	59
H(1B)	-5039	1090	4897	63
H(1C)	-3506	916	6012	63
H(1)	-6710(80)	2060(30)	2920(40)	79
H(2)	-7160(90)	2780(30)	3540(40)	79

Table 2.14: Torsion angles [°] for complex 4.

N(1)-Cu(1)-N(4)-C(4)	-8(16)
N(3)-Cu(1)-N(4)-C(4)	-12.3(3)
N(2)-Cu(1)-N(4)-C(4)	161.3(3)
N(4)-Cu(1)-N(3)-C(3)	-16.2(3)
N(1)-Cu(1)-N(3)-C(3)	163.8(3)
N(2)-Cu(1)-N(3)-C(3)	-110.0(13)
Cu(1)-N(4)-C(4)-C(3)	38.0(5)
Cu(1)-N(3)-C(3)-C(4)	40.9(5)
N(4)-C(4)-C(3)-N(3)	-52.4(5)
N(4)-Cu(1)-N(1)-C(1)	159(16)
N(3)-Cu(1)-N(1)-C(1)	163.4(3)
N(2)-Cu(1)-N(1)-C(1)	-10.3(3)
N(4)-Cu(1)-N(2)-C(2)	162.1(3)
N(1)-Cu(1)-N(2)-C(2)	-18.0(3)
N(3)-Cu(1)-N(2)-C(2)	-104.8(13)
Cu(1)-N(2)-C(2)-C(1)	42.3(4)
Cu(1)-N(1)-C(1)-C(2)	36.3(4)
N(2)-C(2)-C(1)-N(1)	-52.1(5)

Table 2.15: Hydrogen bonds for complex 4 [Åand °].

D-H...A	d(D-H)	d(H...A)	d(D...A)	<(DHA)
O(1)-H(1)...Br(2)	0.93(4)	2.33(4)	3.250(4)	172(5)
O(1)-H(2)...Br(1)#1	0.77(5)	2.53(5)	3.289(3)	166(6)
N(1)-H(1D)...Br(1)#1	0.9	2.54	3.417(4)	164.2
N(1)-H(1A)...O(1)#2	0.9	2.36	3.169(5)	149.1
N(4)-H(4D)...Br(1)#3	0.9	2.56	3.459(4)	173.5

2.4.2 DNA binding

Experimental absorption titration spectra were carried out at pH 7.2 buffer solution of a Tris–HCl [5 mMTris–HCl, 50 mMNaCl] and with a Cu(II) complex concentration of 5.0 x 10^{-5} M. CT-DNA concentrations were varied between 0 and 1.0 ×10^{-4} M by keeping the total volume of mixture constant to 10.0 mL. The mixed solution of Cu(II) and CT-DNA was

allowed to equilibrate for 10 min at room temperature for each trial before being subjected to absorption measurements [48-53].

2.4.3 Biological assays

2.4.3.1 Preparation of stock solutions

A solution was made by dissolving 20 mg of each complex in 20 mL of Roswell Park Memorial Institutemedia (RPMI) supplemented with 1% non-essential amino acid, 1% l-glutamine, 1% penicillin streptomycin, and 1% amphotericin B. This solution has a concentration of 0.5 mg/mL and was stored at 4 ºC until needed.

2.4.3.2 Cell lines

Human colon cancer cells (HCT116, ATCC number: CCL-247, human, from the epithelial tissue of the colon), human prostate cancer cells (PC3, ATCC number: CRL-1435, human, from human prostate), and human liver cancer cells (HepG2, ATCC number: HB-8065, human, from the epithelial cells of the liver) were grown in Dulbecco's modified Eagle's medium (DMEM) supplemented with 10% fetal calf serum, 1% non-essential amino acid, 1% l-glutamine, 1% penicillin streptomycin and 1% amphotericin B. All cell lines were incubated at 37 ºC in a humidified atmosphere of 95% air and 5% CO_2, and the culture medium was changed at least twice a week as needed. All chemicals employed were purchased from biological commercial sources except for the amphotericin B and MTT reagent which were obtained from SIGMA and cell lines purchased from ATCC, USA.

2.4.3.3 Determination of cell viability

Cell viability was assayed by using the MTT method, which is based on the reduction of 3-(4,5-dimethylthiazol-2-yl)-2,5-diphenyltetrazolium bromide (MTT) dye to purple formazan crystals by mitochondrial succinate dehydrogenase enzyme in living cells (47). The cells were seeded into 96-well plates at a density of 1 x 10^4 cells/well and allowed to incubate for 24 h. Cells were then incubated with increasing concentrations of test compounds for another 24 h. At the end of each treatment period, 10 μL of MTT (5 mg/mL in PBS) was added to each well and the microplate was incubated at 37 °C for 4 h. The medium with MTT was removed and 100 μL of Dimethyl sulfoxide (DMSO) was added to each well to dissolve the insoluble formazan crystals. Plates were incubated for 20 min at 37 °C and optical densities were measured at 570 nm with a reference wavelength of 630 nm as a background using a spectrophotometer plate reader.

Cell viability was defined as a percentage of absorbance of treated cells to the control.

2.4.3.4 In vitro cell growth inhibition assay (MTT assay)

Cells were seeded in 96-well plates at a concentration of 1 × 10^4 cells/well in 100 μL of complete media and incubated for 24 at 37 °C in a 5 % CO_2 atmosphere to allow for cell adhesion. Stock solutions (1 mg/mL) of compounds **1** and **2** made in PBS were filter-sterilized, then were further diluted by incomplete media for treatment against cell lines to achieve the following concentration: 1, 0.5, 0.250, 0.125, 0.065, and 0.03125mg/mL. A

100 µL solution of each compound was added to a 100 µL solution of fresh medium in wells to give final concentrations of 1–0.03125 mg/mL. All assays were performed in triplicates. A control group containing no drug was run in each assay. After 24 h exposure of cells to compounds **1** and **2**, each well was carefully rinsed with 200 µL of PBS buffer. Cytotoxicity was assessed using MTT solutions (5 mg/mL) and 100 µL of fresh, complete media which were added to each well. Following a four hour incubation, the medium was removed and the purple formazan precipitated in each well was sterilized in 100 µL DMSO. Absorbance was measured by means of a microplate reader (molecular device) at 570 nm and results are expressed as IC_{50} values directly calculated from % viability (directly proportional to metabolic active cell number). Percentage (%) viability was calculated according to the following equation:

% viability = (OD in sample well/OD in control well) × 100% (OD = optical density)

Chapter Three
Results and Discussion

3.1 Background

Propylenediamine is an excellent primary diaminecomplexing reagent and acts as an N,N-bidentate ligand is capable of coordinating with most of transition metal ions, including Cu(II) [22,23]. Diamine-Cu(II) complexes were found to serve as catalysts under mild conditions [24,25]. In addition, copper(II) complexes containing polydiamine ligands have shown high anti-cancer activity which may be due to their ability to inhibit DNA synthesis [27-35]. Recently, we have investigated the spectroscopic and the biological activity of $[Cu(dipn)(N\text{-}N)]Br_2$ with [dipn = dipropylenetriamine, N-N = ethylenediamine (en) and propylenediamine (pn)] [23].

Although copper complexes have important biological and chemotherapeutic activities, little is known about mono-cationCu(II)-diamine complexes in the solid state X-ray single crystal analysis [29-34]. In view of the broad interest in this type of copper(II) complexes, and owing to their biological importance, we describe herein the preparation, characterization, X-ray structure, and surface studies of new water soluble mono-cation$[CuX(N\text{-}N)_2]^+X^-$complexes (X^- = Cl^- and Br^-). In addition, the antitumor activity of the desired complexes against different cancer cell lines has been investigated.

3.2 Synthesis of aqua bromo-bis-(1,3-diamine)copper(II) bromide complexes 1-4

As shown in **Scheme3.1**, copper(II) complexes, with the general formula $[CuX(N\text{-}N)_2]X$, were prepared by reaction of1,2-ethylenediamine/ 1,3propane--diamine with a copper(II) halide in an ethanol-water mixture and in a 2:1 ligand -to-metal ratio. The complexes have been prepared, in good yields, as water-soluble chloride and bromide salts, respectively. Furthermore, these complexes were blue in color and the reactions that led to their formation were highly exothermic. These newly synthesized complexes were characterized by elemental and spectral analysis.

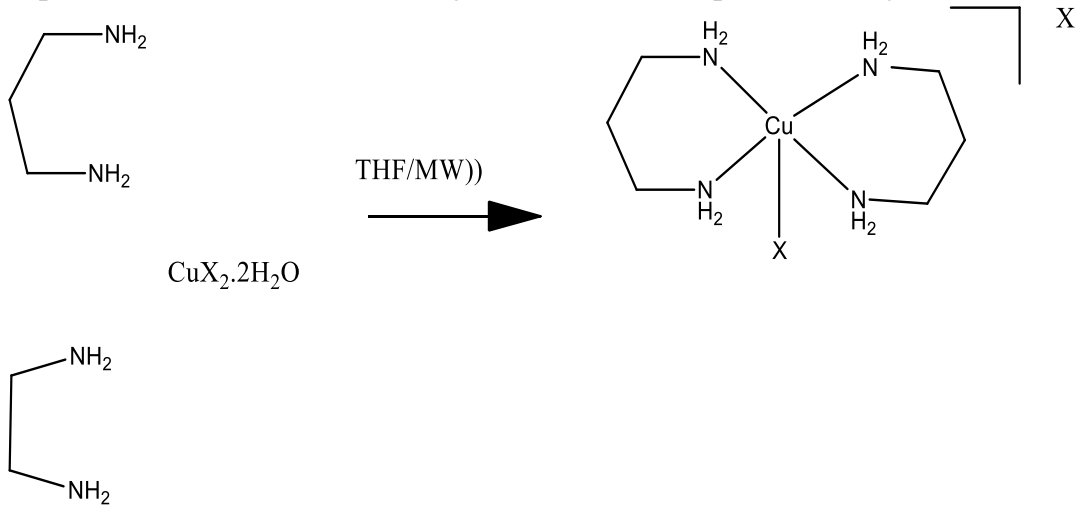

X = Cl (complex **1**), Br (complex **2**)

Scheme 3.1: Synthesis of complexes **1,2,3** and **4**.

3.3 Crystal structure determination and Hirshfeld surfaces analysis

Complex **2** contains a mononuclear copper(II) complex mono-cation, bromide ion (Br13), and a dehydrated water molecule (O14) as depicted in **Figure 3.2.**

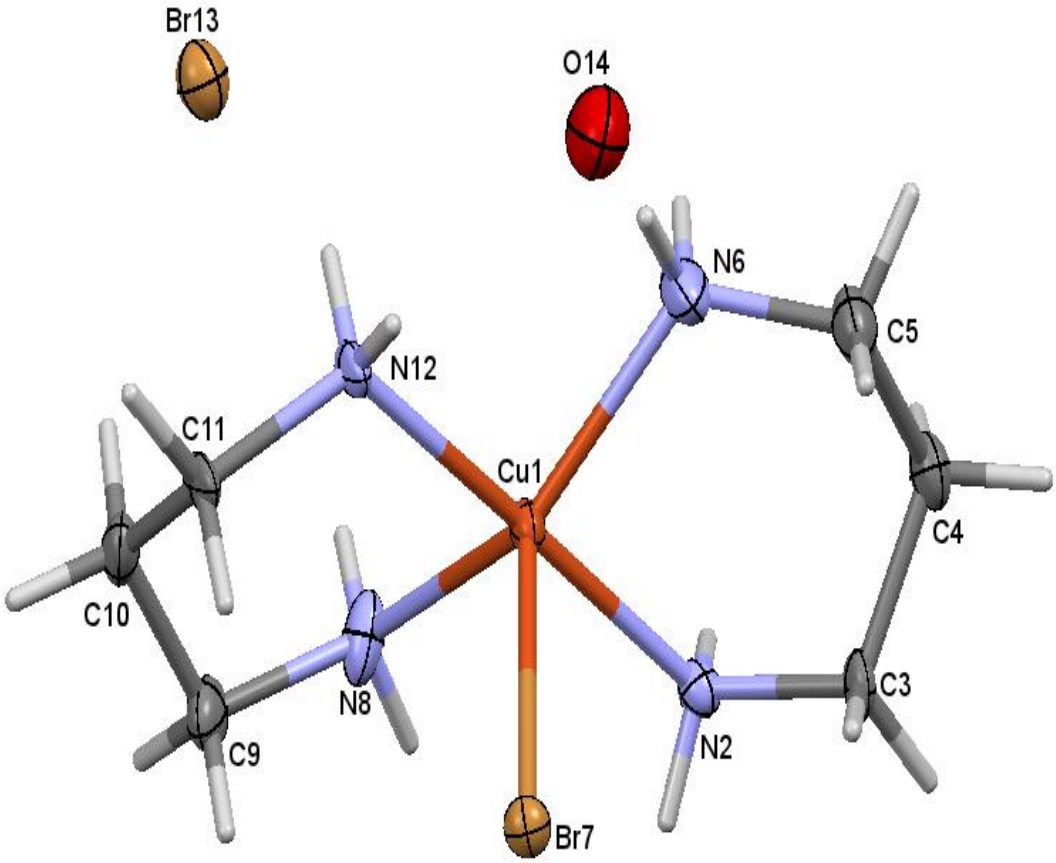

Figure 3.2: ORTEP diagram of complex **2** with thermal ellipsoids drawn at 50% probability.

For this complex, the central Cu(II) ion coordinates with four nitrogen atoms (N2, N6, N8, and N12) and one bromide ion (Br7) and attains a square pyramidal (CuN4Br) coordination geometry. An intramolecular hydrogen bond C11---H11B…Br7 with a distance of 3.584 (4) Å (angle 127^0) is observed. Furthermore, the intermolecular hydrogen bonds N2---H2A…Br7 (distance = 3.476 (3) Å, angle = 155^0 and symmetry = *1-x,1-y*, -

z), N2---H2B…Br13 (distance = 3.533 (3) Å, angle = 161^0 and symmetry = *1-x,1-y, -z*), N6---H6B…Br7 (distance = 3.399 (4) Å and angle = 130^0), N8---H8B…Br7 (distance = 3.550 (4) Å, angle = 154^0 and symmetry = *x,3/2-y, -1/2+z*), N12---H12A…Br13 (distance = 3.569 (3) Å, angle = 127^0 and symmetry = *x,3/2-y,1/2 -z*) and N6---H6A…O14 (distance = 2.990 (6) Å, angle = 152^0 and symmetry = *1-x,1-y,1-z*) connect the molecules in 3D architecture (**Figure3.3** along a, along b, along c) in the crystal packing.

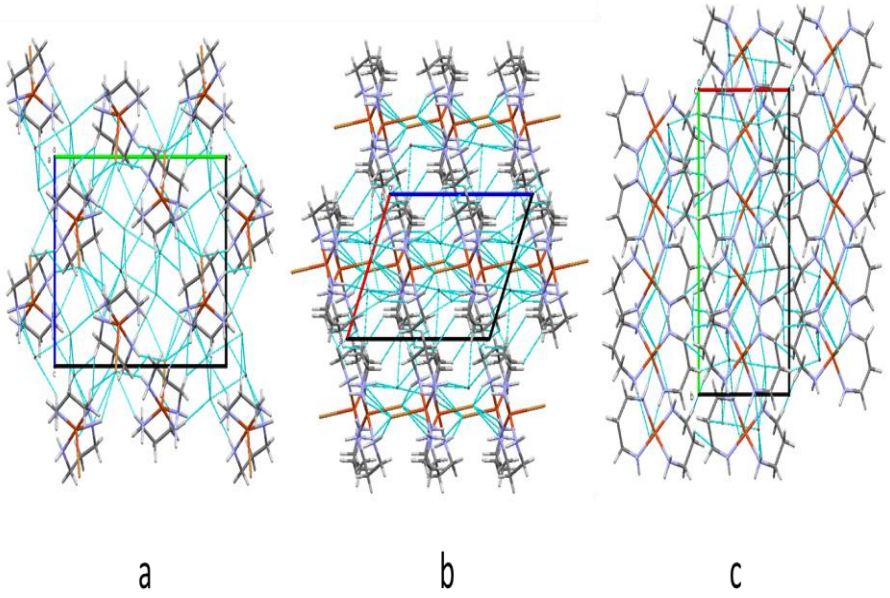

Figure 3.3: Molecules packing viewed down along the *a*-, *b*-, and *c*-axis.

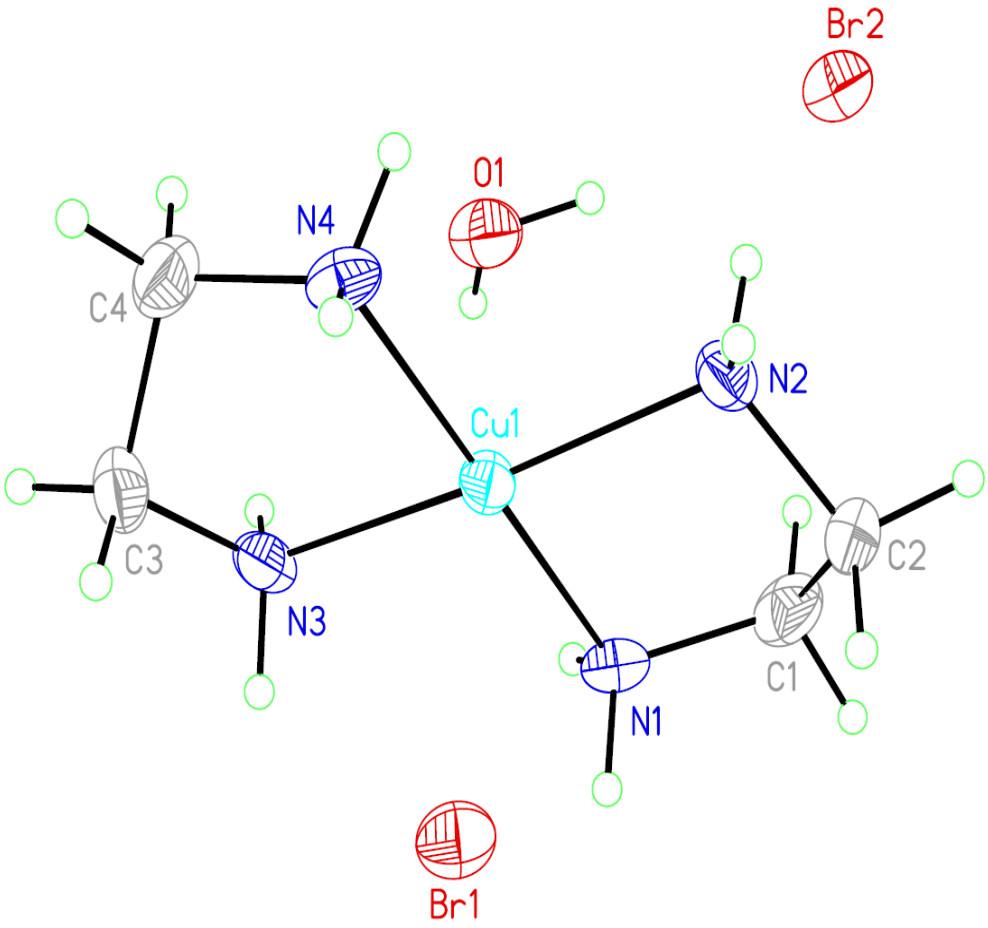

Figure 3.4: ORTEP diagram of complex **4** with thermal ellipsoids drawn at 50% probability.

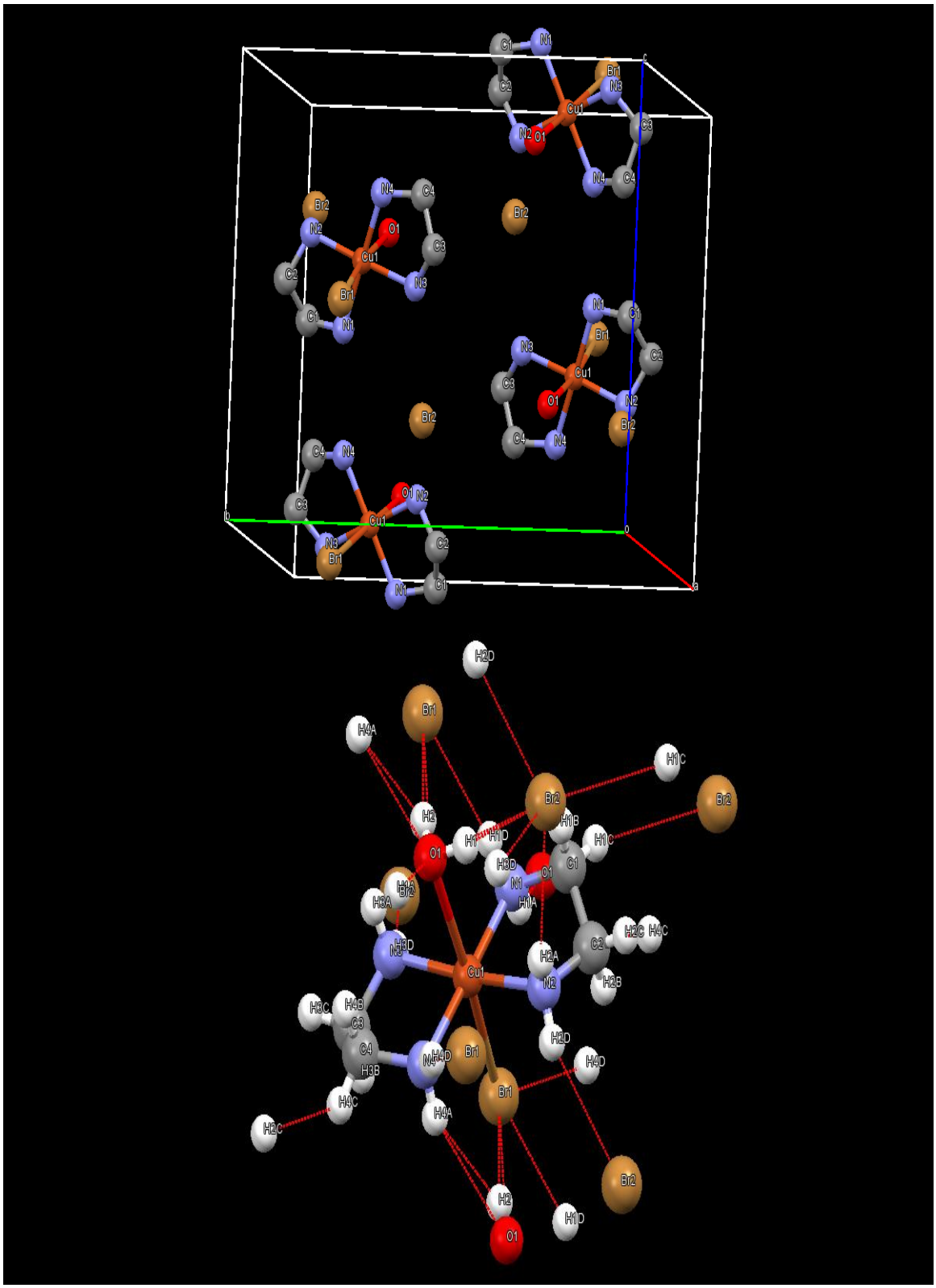

Figure 3.5: Above: Molecules packing viewed down along the *a*-, *b*-, and *c*-axis,**down**:

Molecules interactions viewed

Displayed in Figure **3.6** is the Hirshfeld surface of compound **2**. Hydrogen bonds and other sufficient intercontactswere indicated by red spots over whole molecule surface [40,41]. The dark-red one spots on the d_{norm} appear as a result of the short interatomic contacts, whereas long interactions raise as light-red spots.

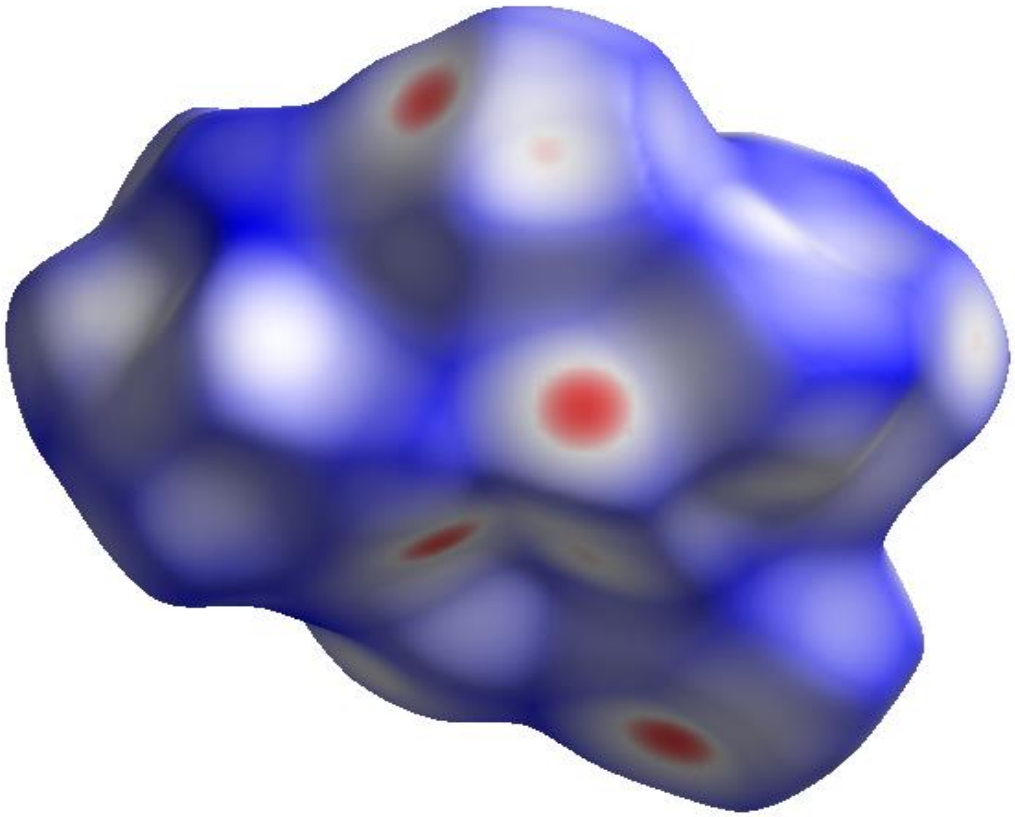

Figure 3.6: Hirshfeld surface d_{norm} map visualizing the complex **2** intercontacts. Color scale in between −0.18 au (blue) to 1.4 au (red).

The 2D Finger print plots over the Hirshfeld surfaces show the presence of intercontacts H…H (52.8 %), H…Br (32.7 %), H…O (12.4 %) and Br…O (2.1 %) (Figure 3.7). The major contribution, however, comes from H…H whereas the least contribution arises from Br…O.

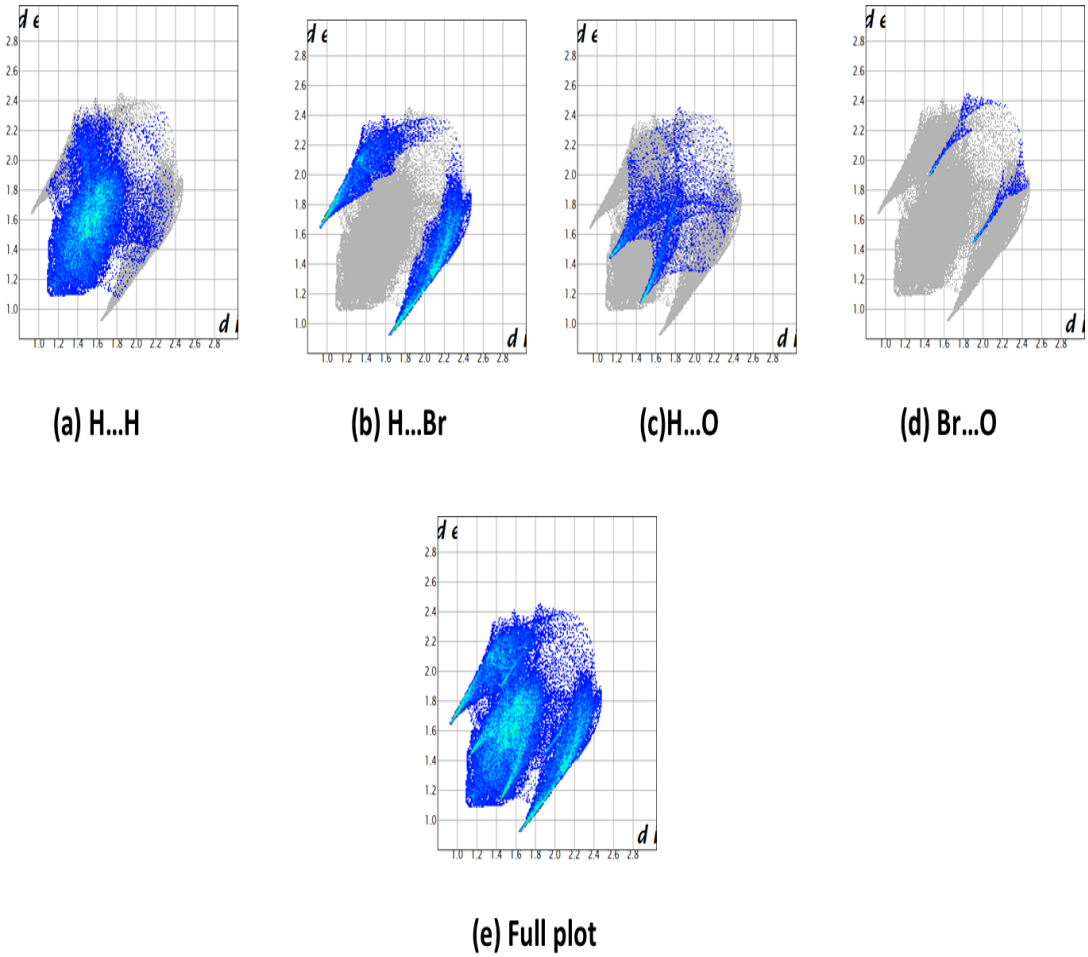

Figure 3.7 Fingerprint of complex **2**, (a) H...H, (b) H...Br, (c) H...O, (d) Br...O, and (e) Full.

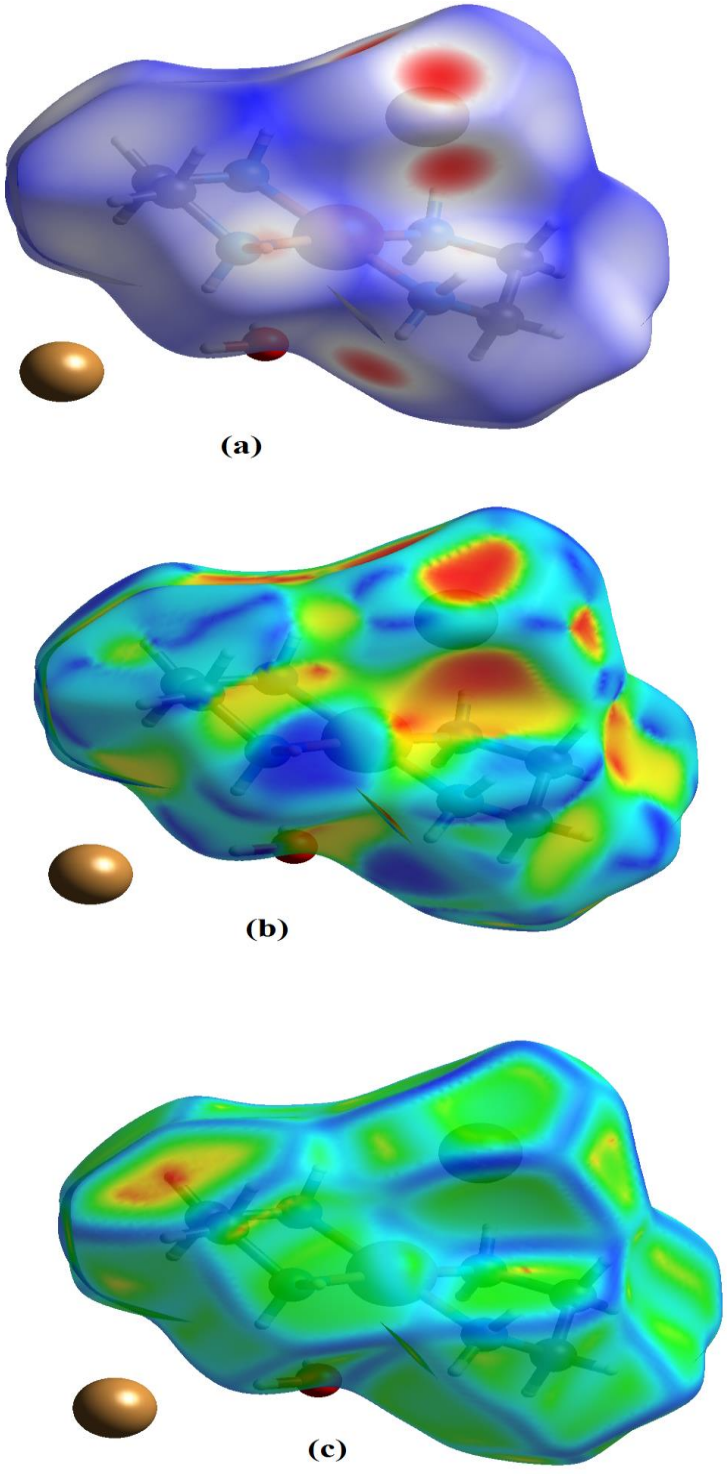

Figure 3.8: Hirshfeld surface d_{norm} map visualizing the complex **2**intercontacts. Color scale in between −0.28 au (blue) to 1.21 au (red).

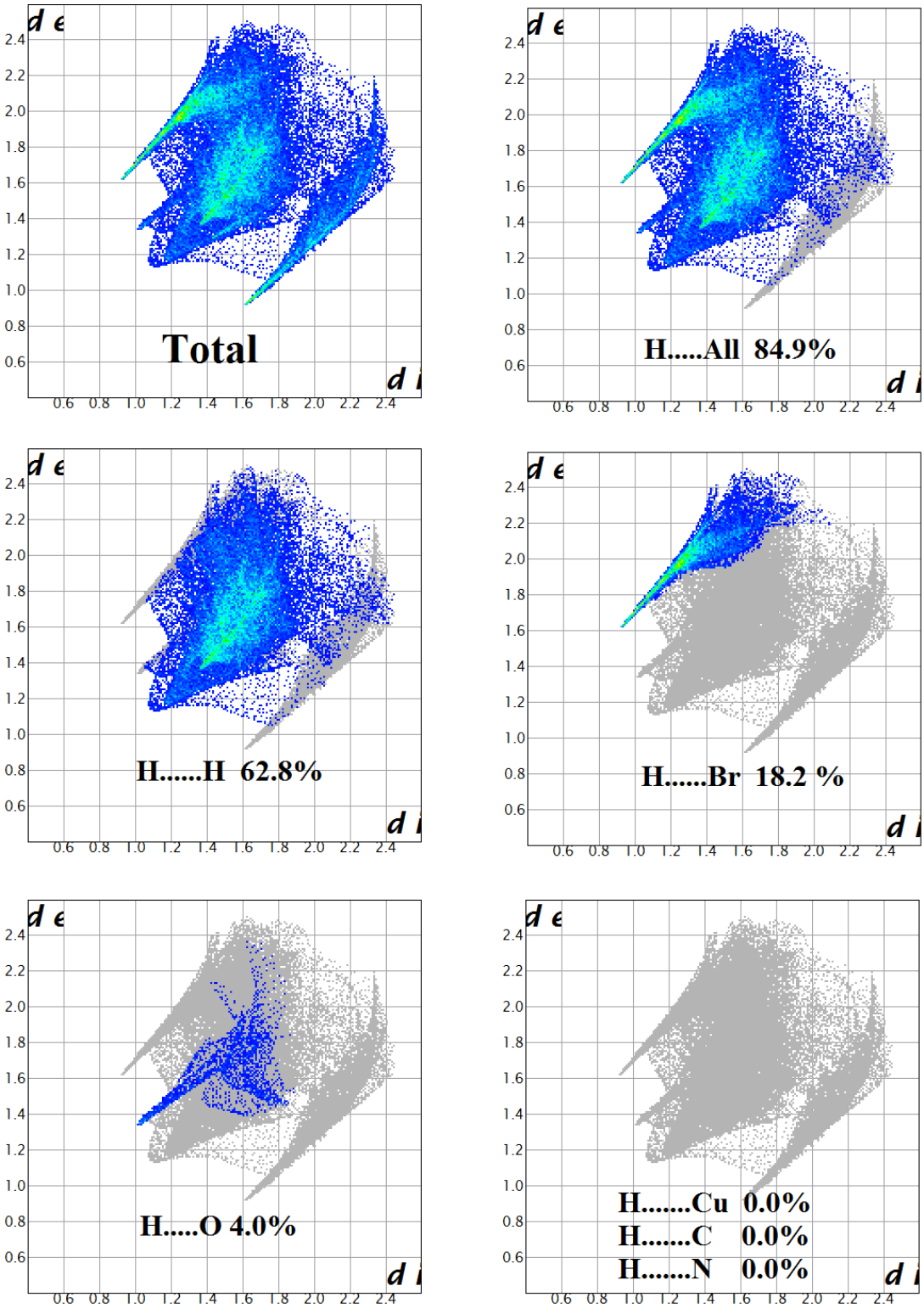

Figure 3.9: Fingerprint of complex **4.**

3.4 Elemental analyses and mass spectrum

The mass spectrum and elemental analysis of the desired complexes are consistent with their proposed molecular formula. As an example complex **2**: Calc. for $C_6H_{20}Br_2CuN_4$: C, 19.39; H, 5.42; N, 15.08. Found: C, 19.15; H, 5.21; N, 14.92%. TOF-MS of **2** is in agreement with its structure showing $[M^+]$ = 292.2 *m/z*, (290.4 theoretical) as in **Figure 3.10**.

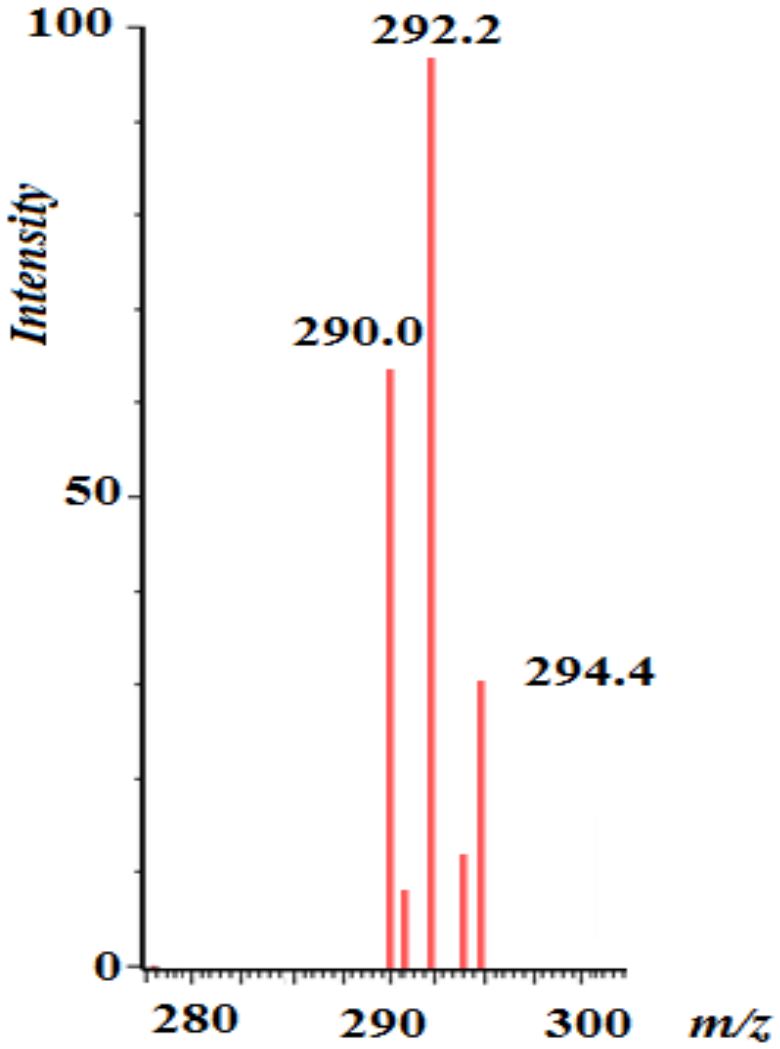

Figure 3.10: TOF-MS spectrum of complex 2.

3.5 FT-IR spectral analysis

The FT-IR of complexes showed similar behavior, IR of **1** and **2** are given in **Figure 3.11** IR spectra revealed strong absorption bands in 3300–3200 and 1650–1520 cm^{-1} assigned to ν_s/ν_{as} (N–H) and ν_b(N–H), respectively; such bands are slightly shifted to lower wavenumbers, and are sharper than those of the free primary diamine, indicating the coordination of the $–NH_2$ groups with Cu(II) center. The strong bands in the range 2950-2850 cm^{-1} are attributed to the C-H stretching vibrations of sp^3 CH_2 groups in the diamine ligand [43]. In addition, the band at 610-500 cm^{-1} is assigned to $\nu_{(Cu-N)}$ vibrations [44,45].

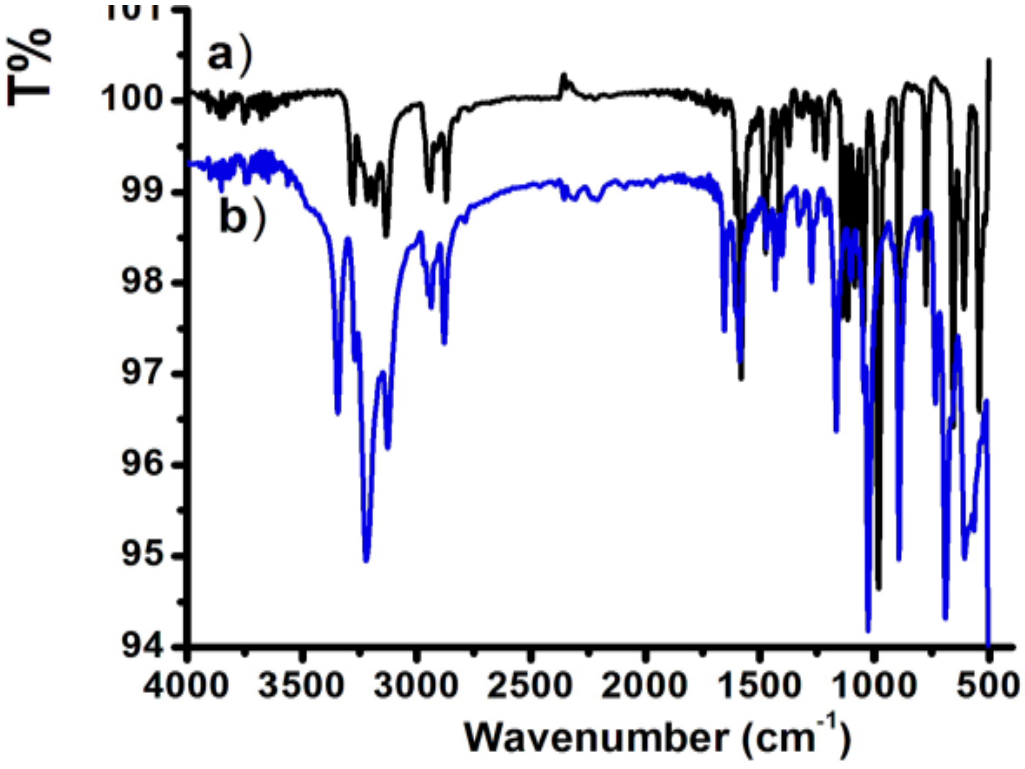

Figure 3.11 The FT-IR spectra of complex **1** a) and complex **2** b).

3.6 UV-Vis. spectral analysis

Complexes **1** and **2** UV-Vis. spectra were recorded in distilled water at room temperature. The complexes exhibited absorption bands at λ_{max} = 250 nm (complex **1**) and 255 nm (complex **2**), as seen in **Figure 3.12**, corresponding to π-π* transition. Additionally, the absorption bands at λ_{max} = 580(complex **1**) and 568 nm (complex **2**), in the blue color region are due to the d-d electronic transition [29-33].

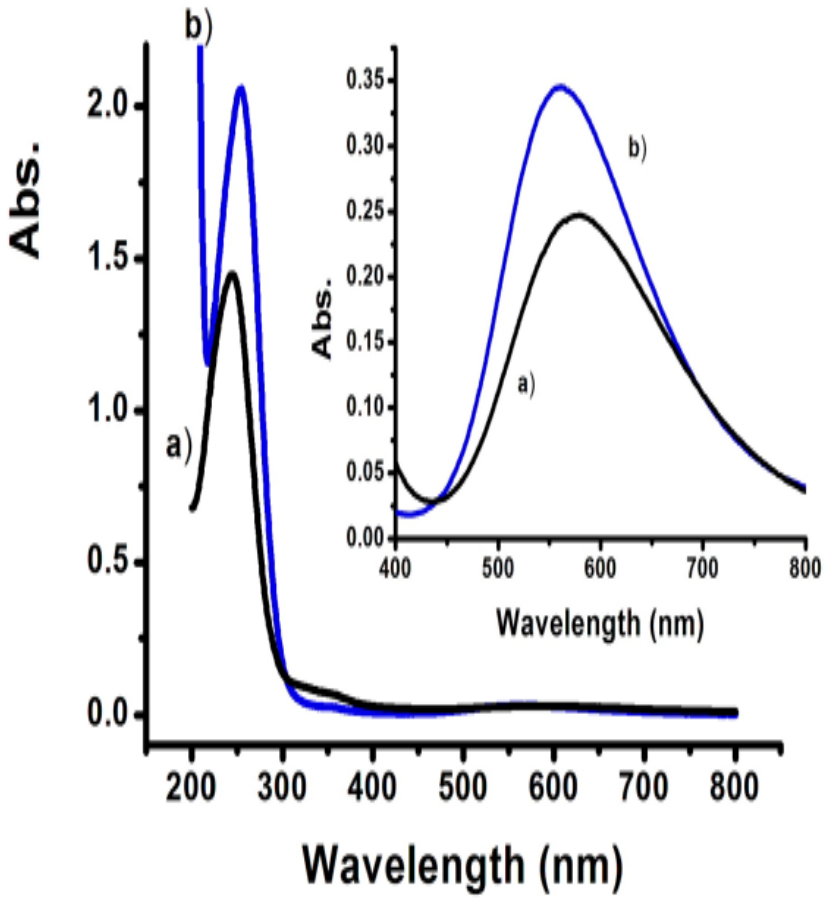

Figure 3.12: UV–Visible spectra of 1 x 10^{-4} M: a)**1**, and b) **2**in H_2O and at room temperature.

3.7 Solvatochromism

Solubility of the newly prepared complexes in polar solvents limits the number of solvents which can be used to evaluate the solvatochromism phenomena in these compounds. For this reason, we have used H_2O, EtOH, DMF, and DMSO in this investigation. Vis. Absorption spectra of complex **2** in selected solvents are seen in **Figure 3.13**. The visible spectra of this complex in different solvents reveal absorption bands in the region 420-800 nm. Solvatochromic probes in such solvents are ascribed to strong expected Jahn–Teller effect of copper(II) ion (d^9).

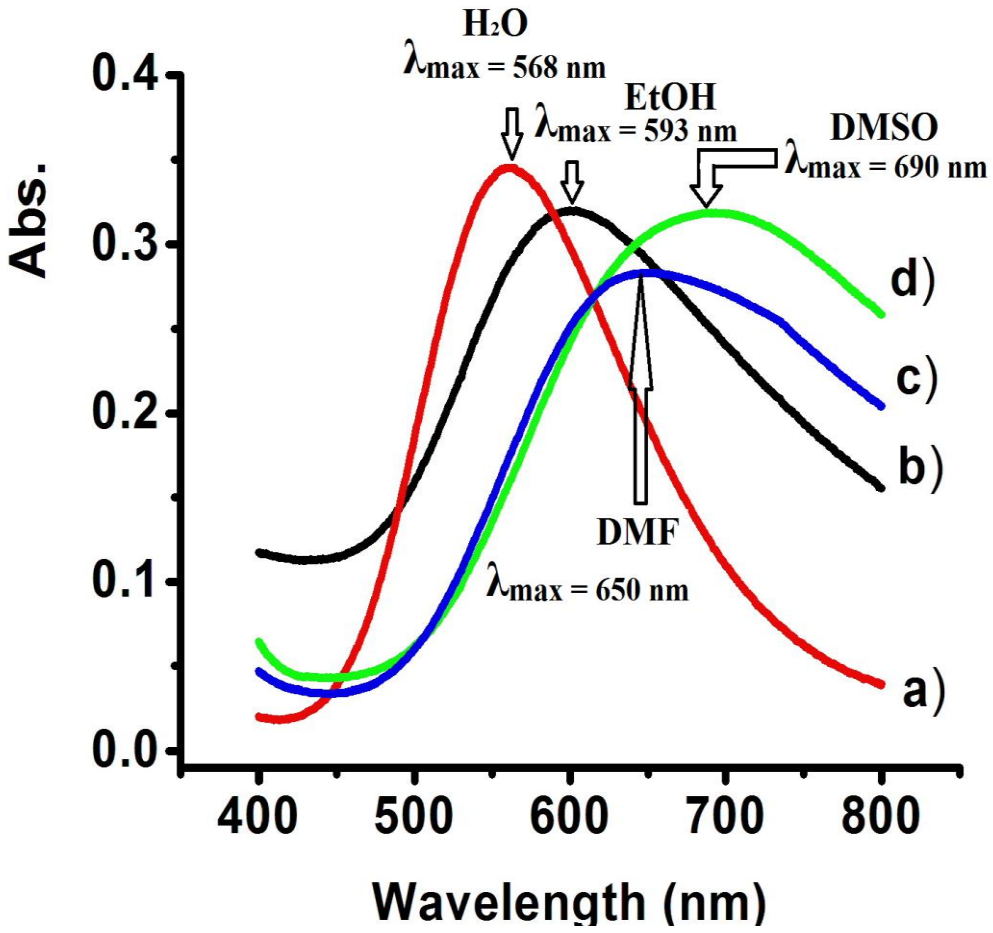

Figure 3.13 Absorption spectra of **2**in selected solvents.

Bathochromic color changes shift was observed and is attributed to the direct coordination of the polar solvent to the vacant sites of the Cu(II) center with different strengths, which is in agreement with the mechanism of solvatochromism behavior of such complexes [46-48].Accordingly, the visible bands chemical shift increases linearly with increasing the Gutmann's donor values (DN) of the solvent. The linear trend of $\lambda_{max}$of complex **2** against DN is presented in **Figure 3.14**.

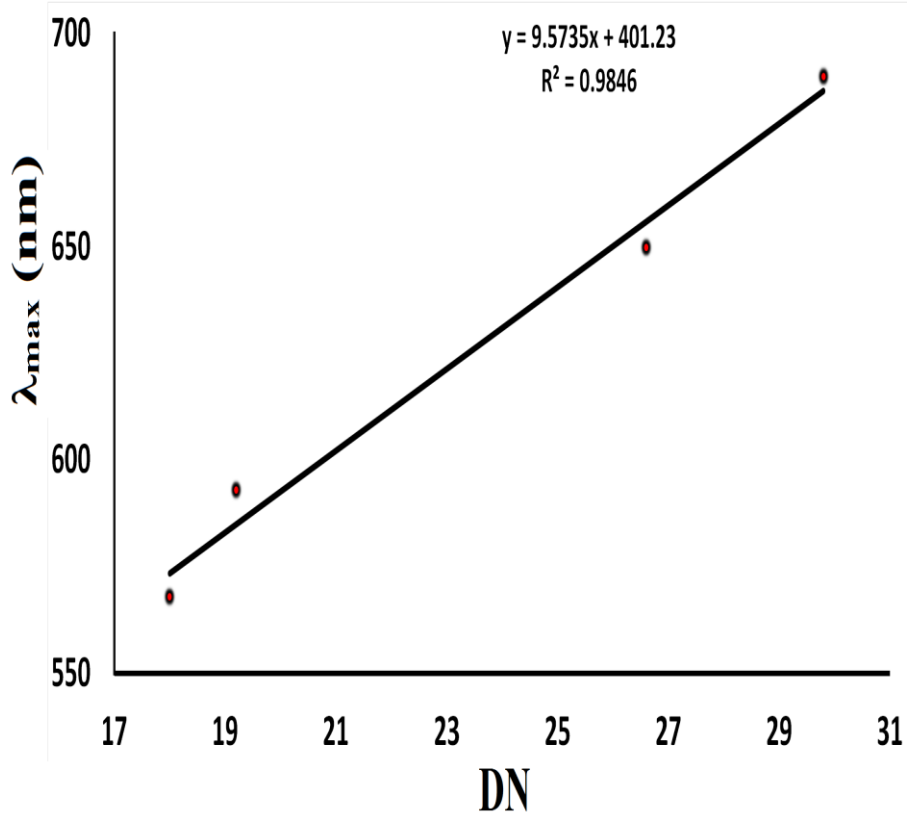

Figure 3.14 Dependence of λ_{max} of complex **2** on the solvent's Gutmann donor number values.

3.8 Thermogravimetric analyses

In the current investigation, we have performed thermal analyses (TG/DTG) to collect information upon stability of complex **4**. To perform these measurements, the temperature was increased from 0 to 900 ^{o}C at a heating rate of 10 ^{o}C min^{-1}. Displayed in **Figure 3.15** are the resulting TGA curves for complex **4**.

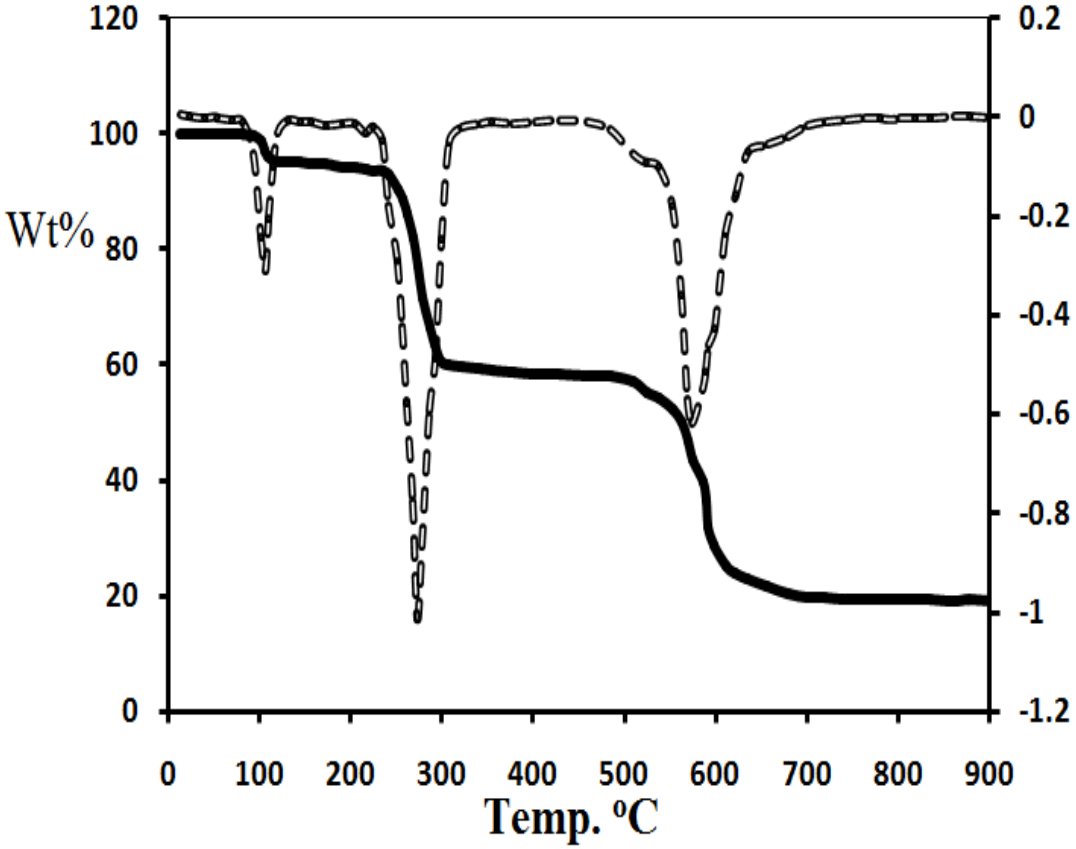

Figure 3.15 TG/DTG thermal curve of complex **4** (TG is the thick solid line, other line represents DTG).

Results from thermogravimetric analysis of the complex revealed the occurrence of three consecutive mass losses; dehydration, organic ligand pyrolysis, inorganic ligand de-structure to metal oxide residue formation.

The first step which involved loss of uncoordinated water molecule was at ~ 100 ^{o}C. In the second decomposition stage, the diamine ligand was lost in the temperature range of 200-280 ^{o}C to form $CuBr_{2.}$ At higher temperatures, the complex undergoes further decomposition that eventually leads to production of copper(II) oxide (CuO); this stage takes place in the temperature range of 580-620 ^{o}C.

3.9 CT-DNA binding

CT-DNA binding affinity of complexes (absorption titration)

UV visible absorption titration spectroscopy is one versatile methods to estimate DNA-binding affinity [48]. The affinity of the complexes toward CT-DNA was followed by UV-visible titrations in Tris–HCl buffer solution. Typically, changes are expected inUV spectra of the desired compound bydrug-DNA binding [51].**Figure 3.16** showing the UV-Visible spectra titration of complex **1** upon CT-DNA addition.

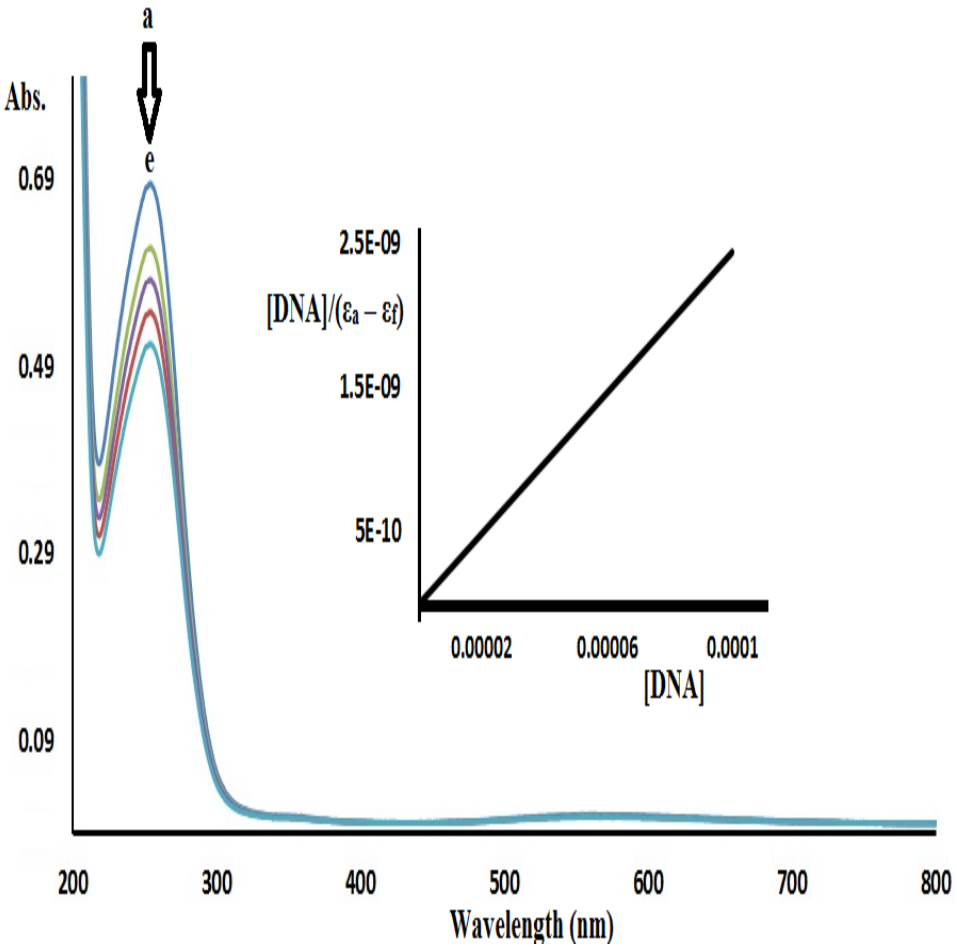

Fig. 3.16: 5.0 ×10^{-5} M of complex **1** UV-Vis. spectra interacted with a) 0, b)1.0 × 10^{-6},c) 5.0 × 10^{-6}, d)1.0 × 10^{5} and e)1.0 × 10^{-4} M (a⟶e) [DNA] at RT. Plot of [DNA]/($\varepsilon_a - \varepsilon_f$) *vs.*[DNA] at λ_{max} = 250 nm to determine the intrinsic binding constant K_b**.**

5x10^{-5} M of the complexes were treated with several DNA concentrations ranging from 0 to 1 x 10^{-4} M in order to monitor the decrease in absorption at λ_{max}= 250nm, as seen in **Figure 3.17**. To evaluate the binding ability of investigated complexes, K_b (intrinsic binding constant) for both complexes was evaluated by observing the changes in Abs. *vis.* CT-DNA concentrations by using the following equation [49-53]:

$$[DNA] / (\varepsilon_a - \varepsilon_f) = [DNA] / (\varepsilon_b - \varepsilon_f) + 1 / K_b (\varepsilon_b - \varepsilon_f)$$

[DNA] is the concentrations of DNA in base pairs, ε_f, ε_a, and ε_b are the free-, apparent-, and metal-bound-complex extinction coefficients, respectively. K_b is the equilibrium binding constant (in M^{-1}) of complex binding to DNA. When plotting [DNA] / (ε_a–ε_f) *vs* [DNA], K_b was obtained from the ratio of the slope to intercept. K_b for complex **1** = 1.30×10^4 M^{-1} (as seen in **Figure 3.16**) and 1.15 x 10^4 M^{-1} for complex **2**. These results are similar to those obtained by other researchers for Cu(II) complexes[49-53].

3.10 Proliferation assay

The MTT cell assay has been widely accepted as a reliable way to measure the cell proliferation rate, and conversely when metabolic events lead to apoptosis or necrosis [47]. Data obtained from the present study by the MTT assay indicated that both complexes have inhibitory effects on the growth of HCT116 colon, HepG2 liver, and PC-3 prostate cancer cells in a dose-dependent manner. In addition, the cytotoxicity of these complexes decreases in a time-dependent fashion. Furthermore, the IC_{50} values for both complexes were found to be 31.25 μg/mL at 24 h of treatment. The importance of such work lies in the possibility that the next generation of metal complexes might be more efficacious as anticancer agents. However, more detailed studies are required to establish the safety and efficacy of these compounds and to have a structure-activity profile for these complexes. Similarly, it is equally important to have an idea about their

stability under biological conditions is required. These detailed investigations could be helpful in designing more potent anticancer agents for therapeutic uses. Furthermore, we performed survival studies where cells were incubated, separately with complexes **1** and **2**, and then washed to remove the metal complexes. The cell survival was determined at complex concentrations ranging from 1 to 0.03215mg/mL). At these concentrations, complex **1** was able to kill 78, 82, 83, 84, 86, and 87% of the HCT116 cells, respectively, as depicted in **Figure 3.17**.

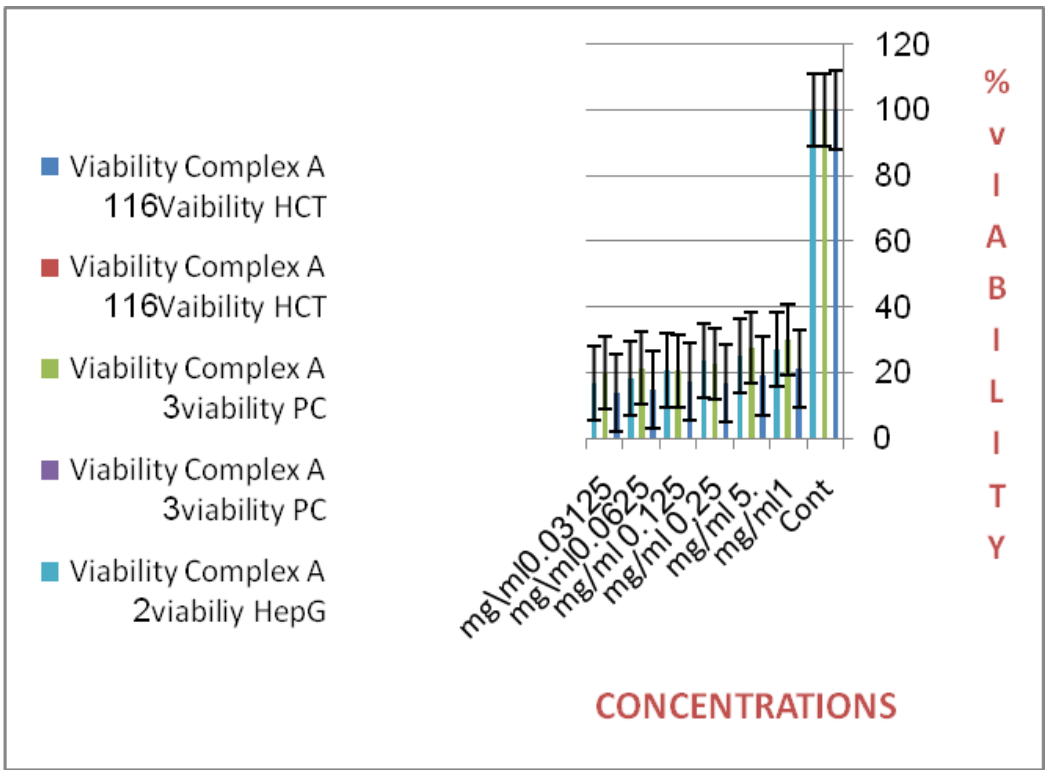

Figure 3.17. Inhibitory effects of complex **1** on the proliferation of HepG2 liver cancer cells, PC3 and HCT 116.

On the other hand, complex **2** at the same concentrations was able to kill 78, 81, 82, 82, 83, and 84 % of the HCT116 cells, respectively, as shown in Figure 3.18.

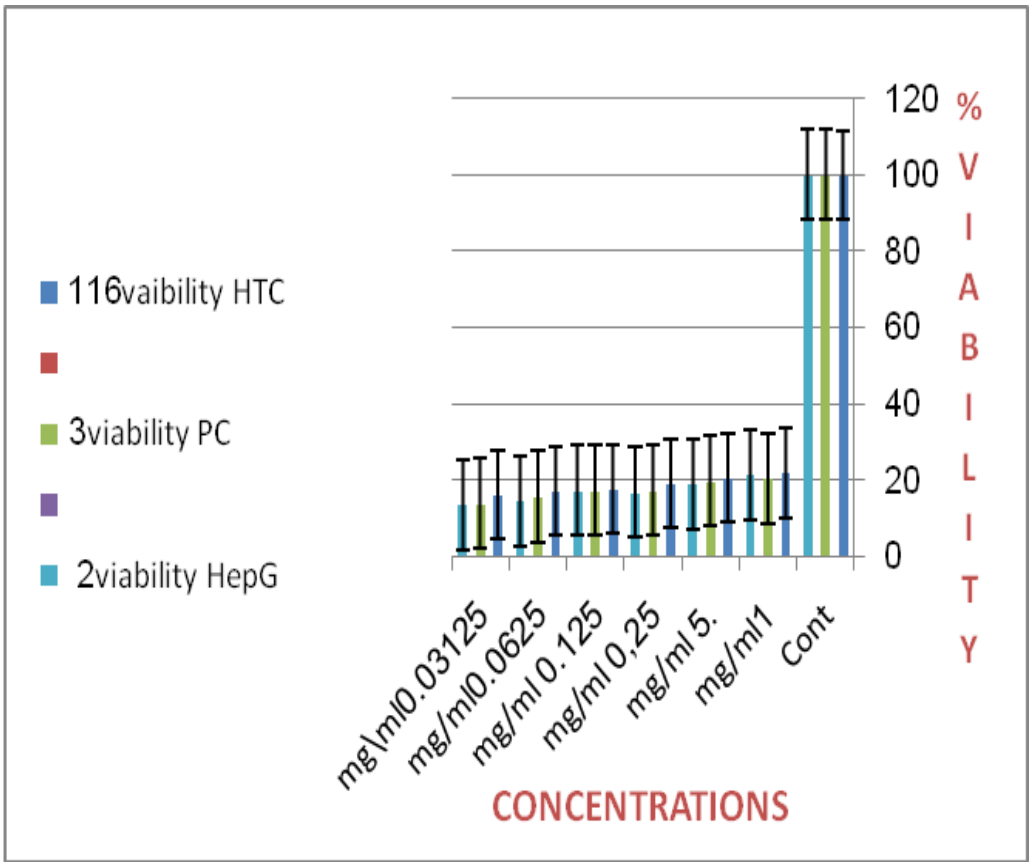

Figure 3.18: Inhibitory effects of complex **2** on the proliferation of HepG2 liver cancer cells, PC3, HCT 11.

Chapter Four

Conclusions

Four new mono-cation propane-1,3-diamines/Cu(II) complexes were prepared and characterized in goodyeilds. The structures of the complexes were determined by several spectral and thermal measurements. Complex **2** demonstrated positive solvatochromism due to coordination of polar solvent molecules with different DNA to the axial site of the Cu(II) center. The single crystal X-ray diffraction data for complex **2** showed that copper ion is in a distorted square pyramid environment. The CT-DNA binding and antitumor activities of the complexes were evaluated; results revealed high CT-DNA binding and antitumor activity against several types of cancer cells.

Supplementary material

Crystallographic data for complex **2** have been deposited with the Cambridge Crystallographic Data Centre as supplementary publication number CCDC 1422015. Copies of this information may be obtained free of charge via www.ccdc.cam.ac.uk/conts/retrieving.html (or from the CCDC, 12 Union Road, Cambridge CB2 1EZ, UK; fax: +44-1223-336033; e-mail: deposit@ccdc.cam.ac.uk).

References

[1] Yamamoto A., ***Organotransition Metal Chemistry***, Wiley, New York, 1990.

[2] Martirosyan, A. Tamazyan, R. Gasparyan, S. Alexanyan, M. Panosyan, H. Martirosyan, V.;Schinazi, ***R.TetrahedronLett***. 51 (2010) 231.

[3] Enders, D.Wortmann, ***L. Heterocycles*** 58 (2002) 293.

[4] Khan, M. Gupta, ***M. Pharmazie*** 57 (2002) 377.

[5] Suzuki, T.Kubota, T. Kobayashi, ***J. Eudistomidins H-K. Med. Chem. Lett***. 21(2011) 4220.

[6] Guggisberg, A. Drandarov, K.; Hesse, ***M.Protoverbine H. Helv. Chim.Acta*** 83(2000) 3035.

[7] Evans, ***R. F. Aust. J. Chem***. 20 (1967) 1643.

[8] Finch, H.; Peterson, E. A.; ***Ballard, S. A. J. Am. Chem. Soc.*** 74 (1952) 2016.

[9] Russowski, D. Canto, R.; Sanches, S. D'Oca, M. Fatima, A. Carvalho, ***J. Bioorg. Chem***. 34 (2006) 173.

[10] Drandarov, K.; Guggisberg, A.; Hesse, ***M. Helv. Chim.Acta*** 82 (1999) 229.

[11] Renson, B. Merlin, P. Daloze, D. Braekman, J. Roisin, Y. Pasteels, ***J. Can. J. Chem***. 72 (1994) 105.

[12] Tu, S. Miao, C. Fang, F. Youjian, F. Li, T.Zhuang, Q. Zhang, X. Zhu, S. Shi, ***D. Bioorg. Med. Chem. Lett***. 14 (2004) 1533.

[13] de Carvalho,G. Dias, R. Pavan, F. Leite, C. Silva, V. Diniz, C. de Paula, D. Coimbra, E. Retailleau, ***P. da Silva, A. Med. Chem***. 9 (2013) 351.

[14] Agbaje, O. Fadeyi, O. Fadeyi, S. Myles, L. Okoro, ***C. Bioorg. Med. Chem. Lett***. 21 (2011) 989.

[15] Hwang, J. Kim, H. Jo, S.; Park, E. Choi, J.; Kong, S. Park, D. Heo, J. Lee, J. Ko, Y. Choi, I. Cechetto, J. Kim, J. Lee, J. No, Z. Windisch, ***M. Eur. J. Med. Chem***.70 (2013) 315.

[16] Billman, ***J. Khan, S. J. Med. Chem***. 9 (1966) 347.

[17] Billman, J. Khan, ***S. J. Med. Chem***. 8 (1965) 498.

[18] Azam, I. Warad, M. Al-Resayes, S. Alzaqri, N. Khan, M. Pallepogu, R.Dwivedi, S. Musarrat, J. Shakir, ***M. J. Molec. Strut***.104 (2013) 48.

[19] Azam, I. Warad, M. Al-Resayes, S. Zahin, M. Ahmad, I. ***Shakir M. Z. Anorg. Allg.Chem***. 638 (2012) 881.

[20] Schmidt, M. Wiedemann, D. Grohmann, ***A. Inorg. Chim.Acta***, 374 (2011) 514.

[21] He, X.-F. Vogels, C. M. Decken, A. Westcott, ***S. A. Polyhedron***, 23 (2014) 155.

[22]Rosu, T. Pahontu, E. Maxim, C. Georgescu, R. Stanica, N. Gulea, ***A.Polyhedron***, 30 (2011) 154-162.

[23] Sathyadevi, P. Krishnamoorthy, P. Alagesan, M. Thanigaimani, K. Thomas, P. Dharmaraj, ***N., Polyhedron***, 31 (2012) 294-306.

[24] Kowalczyk R. Sidorowicz, Ł. Skar_zewski, ***J. Tetrahedron: Asymmetry***, 19 (2008) 2310–2315

[25] Tan, B. Chua, P. J. Li, Y. Zhong, ***G. Org. Lett***.,10 (2008) 2437–2440.

[26] Karvembu, R. Hemalatha, S. Prabhakaran, R. Natarajan, ***K. Inorg. Chem. Commun***., 6 (2003) 486-490.

[27] Mevellec, F. Collet, S. Deniand, D. Reliquet, A. Meslin, ***J.C. J. Chem. Soc.***, 1 (2001) 3128-3131.

[28] Tabassum, S. Amir, S. Arjmand, F. Pettinari, S. Marchetti, F. Masciocchi, N. Lupidi, G. Pettinari, R. Eur. ***J. Med. Chem***.60 (2013) 216–232.

[29] Fu, X.B. Lin, Z.H. Liu, H.F. Le, X.Y., ***Spectrochim.Acta A.***, 122 (2014), 22–33.

[30] Gonzalez-Alvarez, M. Pascual-Alvarez, A. Agudo, L.D. Castineiras, A. Liu-Gonzalez, M. Borras, J. Alzuet-Pina, ***G. Dalton. Trans***. 42 (2013) 10244–10259.

[31] Manikandamathavan, V.M. Rajapandian, V. Freddy, A.J. Weyhermuller, T. Subramanian, V. Nair, B.U. Eur. ***J. Med. Chem***. 57(2012) 449–458.

[32] Song, W-J. Lin, Q-Y. Jiang, W-J. Du, F-Y. Qi, Q.-Y Wei, ***Q. Spectrochim.Acta A.***,137 (2014) 122–128.

[33] Al-Noaimi, M. Nafad, I. Warad, A., Alshwafy, R. Husein, A. Talib, W. H. Ben Hadda,***T. SpectrochimicaActa Part A.***,122 (2014) 273–282.

[34] Al-Noaimi, M. Choudhar, M. I. Awwadi, F. F. Talib, W. H. Ben Hadda, T. Yousuf, A. Sawafta, I. Warad, ***S. SpectrochimicaActa Part A.***, 127 (2014), 225–230.

[35] Wolff, S. K. Grimwood, D. J.McKinnon, J. J. Jayatilaka, D. Spackman, ***M. A. Chemical Communications***,37 (2007) 3814-3816

[36] Bruker, SAINT PLUS, Bruker AXS Inc., Madison, Wisconsin, USA., 2012

[37] Sheldrick, ***G. M. Acta.Cryst.***, A64 (2008) 112.

[38] Spek, ***A. L, Acta.Cryst***., (1990) A46, C34.

[39] Macrae, C. F., Bruno, I. J. Chisholm, J. A. Edgington, P. R. McCabe, P. Pidcock, E.Rodriguez-Monge, L.Taylor, R. van de Streek, J. Wood, ***P.A. J. Appl. Cryst.***, 41 (2008) 466.

[40] McKinnon, J. J. Spackman, M. A. Mitchell, ***A. S. ActaCrystallogr***. B60 (2004) 627–668.

[41] Spackman, M. A. Jayatilaka, **D. Cryst.Engg. Comm**., 11 (2009) 19–32.

[42] Spackman, M. A. & McKinnon, ***J. J. Cryst.Engg. Comm***.4 (2002) 378–392.

[43] C. Tsiamis, C. Themeli, ***M. Inorg.Chim.Acta*** ,206 (1993) 105-115.

[44] Patela, R. Singha, N. Shuklaa, K. Nicl´os-Guti´errezb, J. Astineirasb, S. Vaidyanathanc, V. UnniNairc, ***B. SpectrochimicaActa Part A***.62 (2005) 261–268.

[45] Addison, A. Nageswara-Rao, T. Reedijk, J. Van Rijn, J. Verschoor, ***G. J. Chem.Soc. Dalton Trans.*** (1984) 1349-1356.

[46] El-Ayaan ,U. Murata, F. Fukuda, ***Y. Monatsh. Chem***., 132 (2001) 1279-1284.

[47] Sone, K. Fukuda, Y. Rev., ***Inorg. Chem***. 11 (1990) 123-133.

[48] Linert ,W. Jameson ,R.F. Taha, ***A. J. Chem. Soc. Dalton Trans***. 22 (1993) 3181-3190.

[49] Inamdar, P. Chauhan, R. Abraham ,J**. *Sheela A InorgChemComm***, 67 (2016) 67-71.

[50] Shokohi-pour, Z. Chiniforoshan, H. Abbas , A. Borojeni ,M. Notash, ***B. J. Photochem Photobiology B: Biology***,162 (2016) 34-44.

[51] Pradhan, R. Banik ,M. Cordes, D. Slawin, A. Sah, ***N. Inorg. ChimicaActa***, 442 (2016) 70-80.

[52] Abdel-Rahman ,L.Abu-Dief, A. Ismael, M. Mohamed ,M. Hashem ,***N. J. MolStruc***, 1103 (2016) 232-244.

[53] Jia ,L. Xu ,J. Zhao ,X. ShenSh Zhou, T. XuZh Zhu, T. Chen, R. Ma ,T. Xie ,J. Dong, K. Huang, ***J. J. InorgBiochem***, 159 (2016) 107-119.

جامعة النجاح الوطنية
كلية الدراسات العليا

تحضير وتشخيص طيفي وحراري وكهروكيميائي لعائله جديدة من معقدات النحاس /ثنائي الأمين مع تقييم نشاطها ضد الخلايا السرطانية

اعداد
بهاء عبد الغني

المشرف
أ.د. إسماعيل وراد

قدمت هذه الأطروحة استكمالا لمتطلبات الحصول على درجة الماجستير في الكيمياء، كلية الدراسات العليا، جامعة النجاح الوطنية، نابلس، فلسطين.
2017

تحضير وتشخيص طيفي وحراري وكهروكيميائي لعائله جديدة من معقدات النحاس /ثنائي الأمين مع تقييم نشاطها ضد الخلايا السرطانية

إعداد

بهاء علي عبد الغني

إشراف

أ.د.اسماعيل وراد

الملخص

إن بحثنا تركز على تحضير مركبات جديدة التي من المتوقع ان تدعم كيمياء التنسيق بقوة وامتياز.وأنتجت أربعة مركبات جديدة من مركبات أحادي الايون المائي بوجود العنصر الأساسي النحاس الثنائي Cu(II) مع 1,3- propylenediamine و1,2- ethylenediamine مع كلور أو بروم بروابط في عائد مقبول.وقد تم وصف المركبات طيفيا (الأشعة تحت الحمراء، الأشعة فوق البنفسجية مرئية، وتوف-مس) وكذلك الحرارية (TG/DTA) والتحليل العنصري.

تم إثبات التركيب ثلاثي الأبعاد للمركبات 2،4 من خلال دراسات حيود الأشعة السينية، والتي تبين أن Cu(II) يتم تنسيقها بواسطة أربع ذرات نيتروجين و أيون بروم أو أيون كلور.

في التركيب البلوري ترتبط الجزيئات من خلال تفاعلات ثنائي القطب بين الجزيئات من النوع – N H -- ... Br وروابط هيدروجينية N --- H ... O ، بالإضافة إلى ذلك فقد لوحظ وجود روابط هيدروجينية داخل الجزيئات من نوع H --- C ... Br ؛ هذه التفاعلات تؤدي إلى تقوية الترابط داخل الكريستال ثلاثية الأبعاد.تم استخدام طريقة حسابية هيرشفيلد لمعرفة الطريقة المتداخلة في التركيب البلوري، وأظهرت البيانات أن الروابط الداخلية من نوع H...H بنسبة (52.8%) و H....Brبنسبة (32.7%)، H ... O بنسبة (12.4 %) و O....Br بنسبة (2.1 %) كما تم رصدها كميا.

وقد تم تقييم النشاط المضاد للورم من المركبات المنتجة، وكشفت النتائج عن نشاط عال مضاد للورم ضد عدة أنواع من الخلايا السرطانية.